

South Dakota State University

Open PRAIRIE: Open Public Research Access Institutional Repository and Information Exchange

Electronic Theses and Dissertations

1972

South Dakota Grain Elevator Location and Cost Analysis

Frederick Lorenz

Follow this and additional works at: <https://openprairie.sdstate.edu/etd>

Recommended Citation

Lorenz, Frederick, "South Dakota Grain Elevator Location and Cost Analysis" (1972). *Electronic Theses and Dissertations*. 4804.

<https://openprairie.sdstate.edu/etd/4804>

This Thesis - Open Access is brought to you for free and open access by Open PRAIRIE: Open Public Research Access Institutional Repository and Information Exchange. It has been accepted for inclusion in Electronic Theses and Dissertations by an authorized administrator of Open PRAIRIE: Open Public Research Access Institutional Repository and Information Exchange. For more information, please contact michael.biondo@sdstate.edu.

MODEL STUDY OF Laterally
Loaded Piles in Sand

BY

JEONG-SHWU LIU

A thesis submitted
in partial fulfillment of the requirements for the
degree Master of Science, Master in
Civil Engineering, South Dakota
State University

1972

MODEL STUDY OF LATERALLY
LOADED PILES IN SAND

This thesis is approved as a creditable and independent investigation by a candidate for the degree, Master of Science, and is acceptable as meeting the thesis requirements for this degree. Acceptance of this thesis does not imply that the conclusions reached by the candidate are necessarily the conclusions of the major department.

Thesis Advisor

Date

Head, Civil Engineering

Date

TABLE OF CONTENTS

	Page
INTRODUCTION	1
<u>General</u>	1
<u>Literature Review</u>	1
Theoretical Development	2
Experimental Investigation	4
<u>Scope</u>	6
ANALYTICAL PROCEDURES	8
<u>Matlock and Reese's Generalized Solutions</u>	8
Elastic Pile Theory	8
Rigid Pile Theory	13
<u>Broms' Combined Solutions</u>	14
Deflections at Working Load	14
Ultimate Lateral Resistance	14
EXPERIMENTAL INVESTIGATION	21
<u>Preparation of Soil</u>	21
<u>Subgrade Modulus</u>	21
<u>Loading Test on the Model Piles</u>	27
Loading Device	27
Lateral Deflection at Ground Surface	29
<u>Strain Gage Attachment</u>	29
OBSERVED PERFORMANCE	31
CONCLUSIONS	57

LIST OF TABLES

Table		Page
1.	NON-DIMENSIONAL COEFFICIENTS FOR $k = n_h \times$	11
2.	SOLUTIONS OF EQUATION 1 FOR $k = n_h \times$	11
3.	PHYSICAL PROPERTIES OF MODEL PILE SPECIMENS	22
4.	LATERAL RESISTANCES, Q , FOR 3/8-INCH ROUND STEEL BARS SURROUNDED BY LOOSE SAND	35
5.	LATERAL LOADS, Q , CORRESPONDING TO $y_g = 0.120$ INCHES FOR 3/8-INCH ROUND STEEL BARS ^g SURROUNDED BY LOOSE SAND	37
6.	LATERAL RESISTANCES, Q , FOR 1/4-INCH STEEL PIPES EMBEDDED IN MEDIUM DENSE SAND	42
7.	LATERAL RESISTANCE, Q , FOR 9/16-INCH ROUND STEEL BARS EMBEDDED IN MEDIUM DENSE SAND	47
8.	ALLOWABLE LATERAL LOADS, Q , CORRESPONDING TO $y_g = 0.100$ INCH FOR 9/16-INCH STEEL BARS EMBEDDED IN MEDIUM DENSE SAND	49

LIST OF FIGURES

Figure		Page
1.	TYPICAL DEFLECTION AND MOMENT CURVES FOR LATERALLY LOADED PILE	9
2.	VARIATION OF SUBGRADE MODULUS WITH DEPTH	9
3.	INFLUENCE CURVES FOR DEFLECTION AND MOMENT OF FREE-HEADED PILE WHEN $k = n_h \times (11)$	12
4.	LATERAL DEFLECTION AT GROUND SURFACE FOR FREE-HEADED PILE (4)	15
5.	ASSUMED DISTRIBUTION OF SOIL REACTIONS	15
6.	SHORT FREE-HEADED PILES DISTRIBUTION OF DEFLECTION, SOIL REACTION AND MOMENT	17
7.	ULTIMATE LATERAL RESISTANCE OF SHORT FREE-HEADED PILES (4)	17
8.	LONG FREE-HEADED PILES DISTRIBUTION OF DEFLECTION, SOIL REACTION AND MOMENT	19
9.	ULTIMATE LATERAL RESISTANCE OF LONG FREE-HEADED PILES (4)	19
10.	TEST TO DETERMINE SUBGRADE MODULUS	24
11.	DETERMINATION OF SUBGRADE MODULUS	25
12.	LATERAL LOAD vs DEFLECTION FOR n_h OF LOOSE SAND	26
13.	LATERAL LOAD vs DEFLECTION FOR n_h OF MEDIUM DENSE SAND	26
14.	PILE LOADING APPARATUS	28
15.	LATERAL LOAD vs DEFLECTION FOR 3/8-INCH ROUND STEEL BAR EMBEDDED IN LOOSE SAND	32
16.	LATERAL LOAD vs DEFLECTION FOR 3/8-INCH ROUND STEEL BAR EMBEDDED IN LOOSE SAND	32
17.	LATERAL LOAD vs DEFLECTION FOR 3/8-INCH ROUND STEEL BAR EMBEDDED IN LOOSE SAND	33

Figure		Page
18.	LATERAL LOAD vs DEFLECTION FOR 3/8-INCH ROUND STEEL BAR EMBEDDED IN LOOSE SAND	33
19.	LATERAL LOAD vs DEFLECTION FOR 3/8-INCH ROUND STEEL BAR EMBEDDED IN LOOSE SAND	34
20.	LATERAL LOAD vs DEFLECTION FOR 3/8-INCH ROUND STEEL BAR EMBEDDED IN LOOSE SAND	34
21.	LATERAL LOAD vs DEFLECTION FOR 1/4-INCH STEEL TUBE EMBEDDED IN MEDIUM DENSE SAND	38
22.	LATERAL LOAD vs DEFLECTION FOR 1/4-INCH STEEL TUBE EMBEDDED IN MEDIUM DENSE SAND	38
23.	LATERAL LOAD vs DEFLECTION FOR 1/4-INCH STEEL TUBE EMBEDDED IN MEDIUM DENSE SAND	39
24.	LATERAL LOAD vs DEFLECTION FOR 1/4-INCH STEEL TUBE EMBEDDED IN MEDIUM DENSE SAND	39
25.	LATERAL LOAD vs DEFLECTION FOR 1/4-INCH STEEL TUBE EMBEDDED IN MEDIUM DENSE SAND	40
26.	LATERAL LOAD vs DEFLECTION FOR 9/16-INCH STEEL BAR EMBEDDED IN MEDIUM DENSE SAND	44
27.	LATERAL LOAD vs DEFLECTION FOR 9/16-INCH STEEL BAR EMBEDDED IN MEDIUM DENSE SAND	44
28.	LATERAL LOAD vs DEFLECTION FOR 9/16-INCH ROUND STEEL BAR EMBEDDED IN MEDIUM DENSE SAND	45
29.	LATERAL LOAD vs DEFLECTION FOR 9/16-INCH ROUND STEEL BAR EMBEDDED IN MEDIUM DENSE SAND	45
30.	LATERAL LOAD vs DEFLECTION FOR 9/16-INCH ROUND STEEL BAR EMBEDDED IN MEDIUM DENSE SAND	46
31.	MOMENT vs DEPTH FOR 1/2-INCH STEEL TUBE EMBEDDED IN MEDIUM DENSE SAND	50
32.	LATERAL LOAD vs DEFLECTION FOR 1/2-INCH STEEL TUBE EMBEDDED IN MEDIUM DENSE SAND	50

Figure		Page
33.	MOMENT vs DEPTH FOR 3/8-INCH SQUARE STEEL BAR EMBEDDED IN LOOSE SAND	52
34.	LATERAL LOAD vs DEFLECTION FOR 3/8-INCHES SQUARE STEEL BAR EMBEDDED IN LOOSE SAND	52
35.	LATERAL LOAD vs DEFLECTION FOR 3/8-INCH ROUND STEEL BAR EMBEDDED IN MEDIUM DENSE SAND	53
36.	LATERAL LOAD vs DEFLECTION FOR 3/8-INCH ROUND STEEL BAR EMBEDDED IN MEDIUM DENSE SAND	53
37.	LATERAL LOAD vs DEFLECTION FOR 3/8-INCH ROUND STEEL BAR EMBEDDED IN MEDIUM DENSE SAND	54
38.	LATERAL LOAD vs DEFLECTION FOR 3/8-INCH ROUND STEEL BAR EMBEDDED IN MEDIUM DENSE SAND	54
39.	LATERAL LOAD vs DEFLECTION FOR 3/8-INCH ROUND STEEL BAR EMBEDDED IN MEDIUM DENSE SAND	55

INTRODUCTION

General

The most common function of piles is to transmit foundation loads which cannot be adequately supported at a certain level down to a depth at which adequate support is available. The classification of piles in terms of loading may be considered as vertically or laterally loaded. The laterally loaded pile is a structural member which sustains transverse loads in a similar way a beam does. The lateral force that the pile foundations is subjected to may be induced by earthquake, water waves, moving vessels, wind force, and lateral earth pressure, etc.

Early techniques for analyzing laterally loaded pile foundations completely ignored the soil resistance; the ends of the piles were treated as either pinned or fixed, and the problem became strictly an exercise in structural mechanics. It was generally recognized that these techniques were extremely conservative. The increase in quantity and size of civil engineering works nowadays has thrown large economic pressure for a more precise knowledge of the behavior of pile foundations subjected to lateral load.

Literature Review

The problem connected to laterally loaded piles can be

cast into two parts: first, those dealing with theoretical development by applying mathematics or mechanics, and second, those dealing with soil behavior and actual pile tests. Both parts have been explored by many previous investigators in the literature.

(1) Theoretical Development

Elastic theory is probably the most commonly used method as a theoretical solution for laterally loaded piles. This theory involves the concept of modulus of subgrade reaction based on Winkler's assumption that a medium may be approximated by a series of infinitely closely spaced independent, elastic springs. Laterally loaded piles can therefore be treated as beam on elastic foundation. After the proper forms of variation of subgrade modulus with depth has been determined, a basic governing equation can be solved, and various physical quantities pertaining to the pile-soil system can be obtained from it.

A comprehensive treatise on the subject of subgrade reaction was presented by Terzaghi (1). According to his paper, subgrade modulus may be assumed to be constant for preloaded clays and to vary directly with depth for granular soils and normally loaded silts and clays.

Generalized solutions for laterally loaded piles were presented by Matlock and Reese (2). A group of non-dimensional parameters were introduced for elastic pile

theory. The basic governing equation for laterally loaded piles was transformed into non-dimensional ones by proper substitution of non-dimensional parameters. After solving for these non-dimensional parameters, various physical quantities pertaining to the pile-soil system could be obtained from them.

The above-mentioned elastic pile theory is not applicable to piles having relatively shallow embedment. Rigid pile theory was also presented by Matlock and Reese as the solution for a short rigid pile (2). By application of statics, various physical quantities inherent to the pile-soil system could be obtained.

Broms brought forth a combined application of elastic theory and ultimate resistance theory for the analysis of the behavior of laterally loaded piles surrounded both by cohesive soil (3) and by cohesionless soil (4). Deflections at ground surface could be checked under working load by assuming a constant subgrade modulus for cohesive soil and a subgrade modulus proportional to depth for cohesionless soil. The soil reactions were assumed to be a constant of $9 C_u D$ below the depth of $1.5D$ from the ground surface and of zero above that depth for cohesive soil and three times the Rankine's passive pressure for cohesionless soil, where C_u is half the unconfined compressive strength of soil and D is the diameter or width of pile. The ultimate

resistance of pile-soil system could then be computed by using laws of statics.

(2) Experimental Investigation

Feagin conducted full-scale tests on single piles as well as pile groups embedded 30 feet in dense sand (5). Timber piles and concrete piles were used. For certain amounts of allowable deflection at the ground surface, the corresponding allowable lateral loads per pile were determined from the observed test results.

McClelland and Focht conducted a test in the Gulf of Mexico to investigate soil modulus for laterally loaded pile (6). A 24-inch pipe was driven to a penetration of 75 feet into a layer of normally consolidated clay. The test revealed that the subgrade modulus varied widely not only with depth, but also with pile deflection. In the normally consolidated clay deposit existing at the test site, the subgrade modulus was found to increase almost linearly with depth for any single applied load. However, the rate of increase became smaller as the load increased.

Prakash conducted a series of model tests on pile groups of various pile spacings embedded in selected fine sand (7). The experimental results of comparative single piles were also reported for each test. Matlock and Reese's generalized solution was used as the analytical approach for comparison with the observed results. Subgrade modulus

increasing proportionally with depth was assumed for the sand soil used. Repeated application of non-dimensional technique was employed to account for the non-linearity between pile deflection and soil resistance. The theoretical results were found to be very close to those of experimental ones. It was also shown that the analytical techniques of Matlock and Reese's generalized solutions applied on single piles could be applied on pile groups as well. Pile spacing greater than 8 pile-diameters in the direction of load and/or 3 pile-diameters normal to the load was noted to be required to eliminate the interaction between individual piles in a pile group.

Alizadeh and Davisson conducted full-scale field tests on single piles for the Arkansas River Project (8). Timber, concrete, and steel piles were tested. The soils at the test site were found to be medium to fine sand and silty sand. The non-dimensional technique of Matlock and Reese's generalized solutions was applied repeatedly for theoretical analysis. For vertical piles, reasonable theoretical approximation was obtained by comparing with the observed results.

Davisson and Salley conducted model tests of groups of piles scaled after the prototype pile foundations for locks and dams on the Arkansas River (9). Dry, fine, fairly uniform sand was used for the tests. Again, repeated

application of the non-dimensional analytical technique of Matlock and Reese's generalized solution was used for theoretical approach. The test on a single pile gave a close approximation between the theoretical and experimental results. The effect of group loading is to decrease the effective value of the coefficient of horizontal subgrade reaction.

Scope

Various theoretical approaches for the solutions of laterally loaded piles have been presented by several previous investigators. Both model tests and full-scale field tests have been carried out, and the results were compared with theoretical values computed by repeated application of non-dimensional technique of Matlock and Reese's generalized solutions (7, 8, 9). Soil subgrade moduli were adjusted successively upon each trial through repeated application of Matlock and Reese's generalized solutions so that the non-linearity between pile deflection and soil resistance could be taken into consideration.

The degree of accuracy of the linear approach of Matlock and Reese's general solutions by using a fixed subgrade modulus to approximate the actual non-linear behavior of laterally loaded piles seems to have been investigated very little. Broms' method has not been employed as an analytical approach to compare with the

experimental results for laterally loaded piles in the literature. Therefore, a study of model tests of laterally loaded piles is here presented to investigate these aspects. The theoretical results of using Broms' method and the linear approach of Matlock and Reese's generalized solutions are compared. The criterion of an infinitely long pile has also been checked through experiments.

Single free-headed piles of various embedment lengths surrounded by loose and medium dense sand passing through No. 4 sieve were tested. The classification of the sand soil used in tests is presented in Appendix B.

ANALYTICAL PROCEDURE

(1) Matlock and Reese's Generalized Solutions

Elastic Pile Theory

The basic equation which governs the equilibrium of a laterally loaded pile has been presented by Hetenyi (10).

The equation is

$$\frac{d^4 y}{dx^4} + \frac{k}{EI} y = 0 \quad (1)$$

in which y is the lateral deflection of pile at depth x below ground surface as shown in Figure 1, EI the flexural stiffness of pile and k the horizontal subgrade modulus. Subgrade modulus is defined as the ratio of the soil reaction P per unit length of pile at a certain depth along the pile to the corresponding lateral deflection of pile at the same depth. It can be expressed as

$$k = \frac{-P}{y} \quad (2)$$

For granular soil the subgrade modulus is assumed to increase proportionally with depth and is defined as

$$k = n_h x \quad (3)$$

where n_h is termed the constant of horizontal subgrade reaction. Figure 2 shows the variations of subgrade modulus with depth. The typical n_h values are presented in Appendix C.

If an applied lateral load, Q_g , and an applied moment,

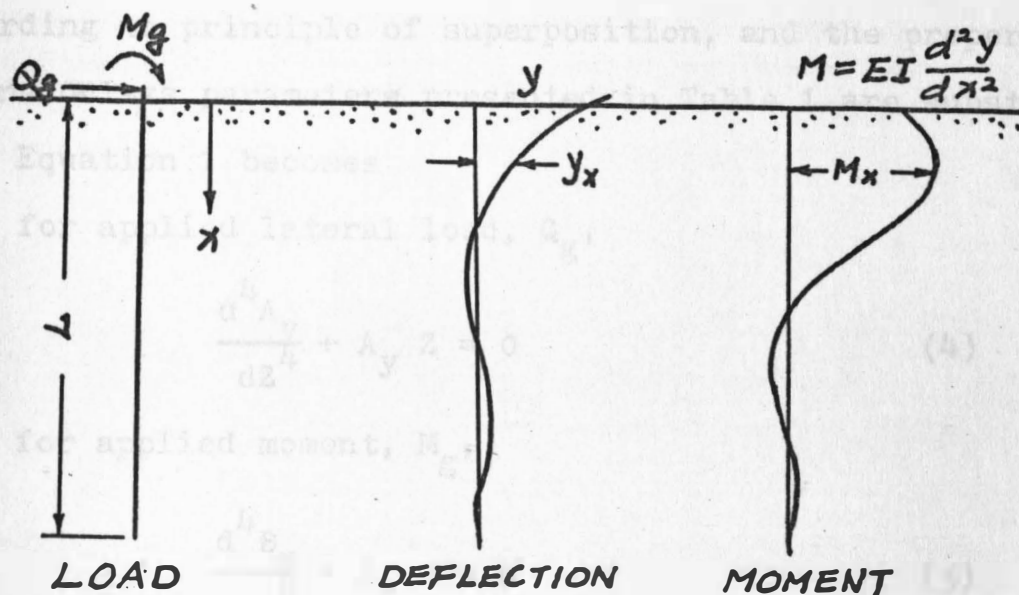


FIGURE 1. TYPICAL DEFLECTION AND MOMENT CURVES FOR LATERALLY LOADED PILE

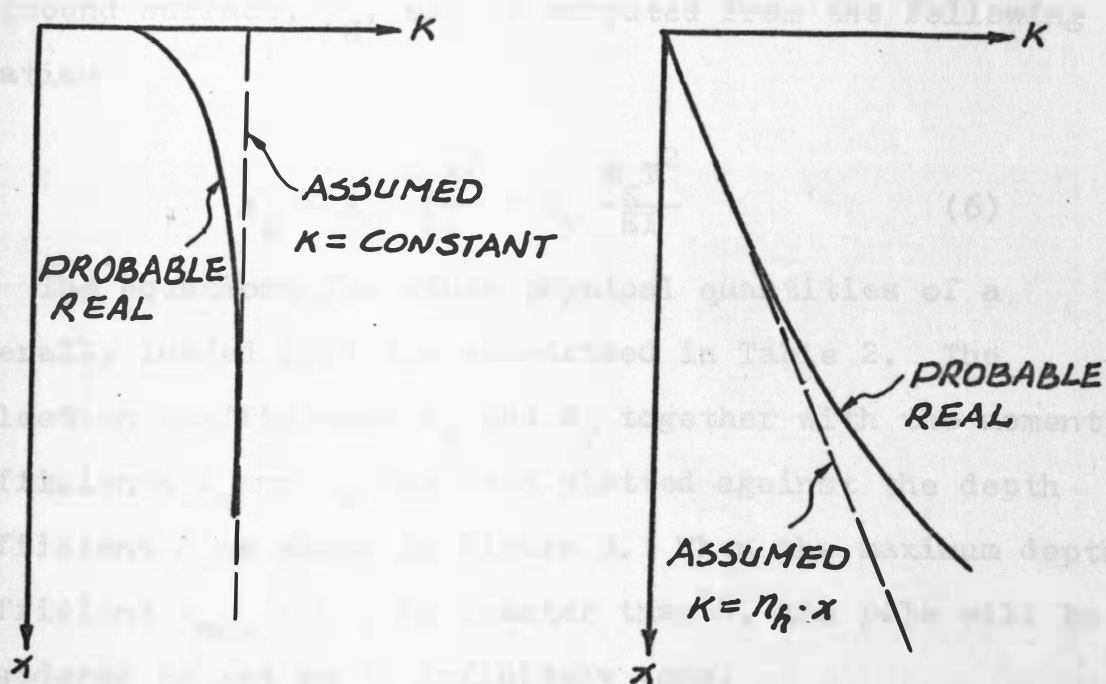


FIGURE 2. VARIATION OF SUBGRADE MODULUS WITH DEPTH

M_g , at the ground surface are considered separately according to principle of superposition, and the proper dimensionless parameters presented in Table 1 are substituted, Equation 1 becomes

for applied lateral load, Q_g ,

$$\frac{d^4 A_y}{dz^4} + A_y Z = 0 \quad (4)$$

for applied moment, M_g ,

$$\frac{d^4 B_y}{dz^4} + B_y Z = 0 \quad (5)$$

Once the dimensionless deflection coefficients A_y and B_y in the above differential equations are solved, the deflection at ground surface, y_g , can be computed from the following equation

$$y_g = A_y \frac{Q_g T^3}{EI} + B_y \frac{M_g T^2}{EI} \quad (6)$$

The equations for other physical quantities of a laterally loaded pile are summarized in Table 2. The deflection coefficients A_y and B_y together with the moment coefficients A_m and B_m has been plotted against the depth coefficient Z as shown in Figure 3. When the maximum depth coefficient $Z_{\max} = L/T$ is greater than 4, the pile will be considered to act as if infinitely long.

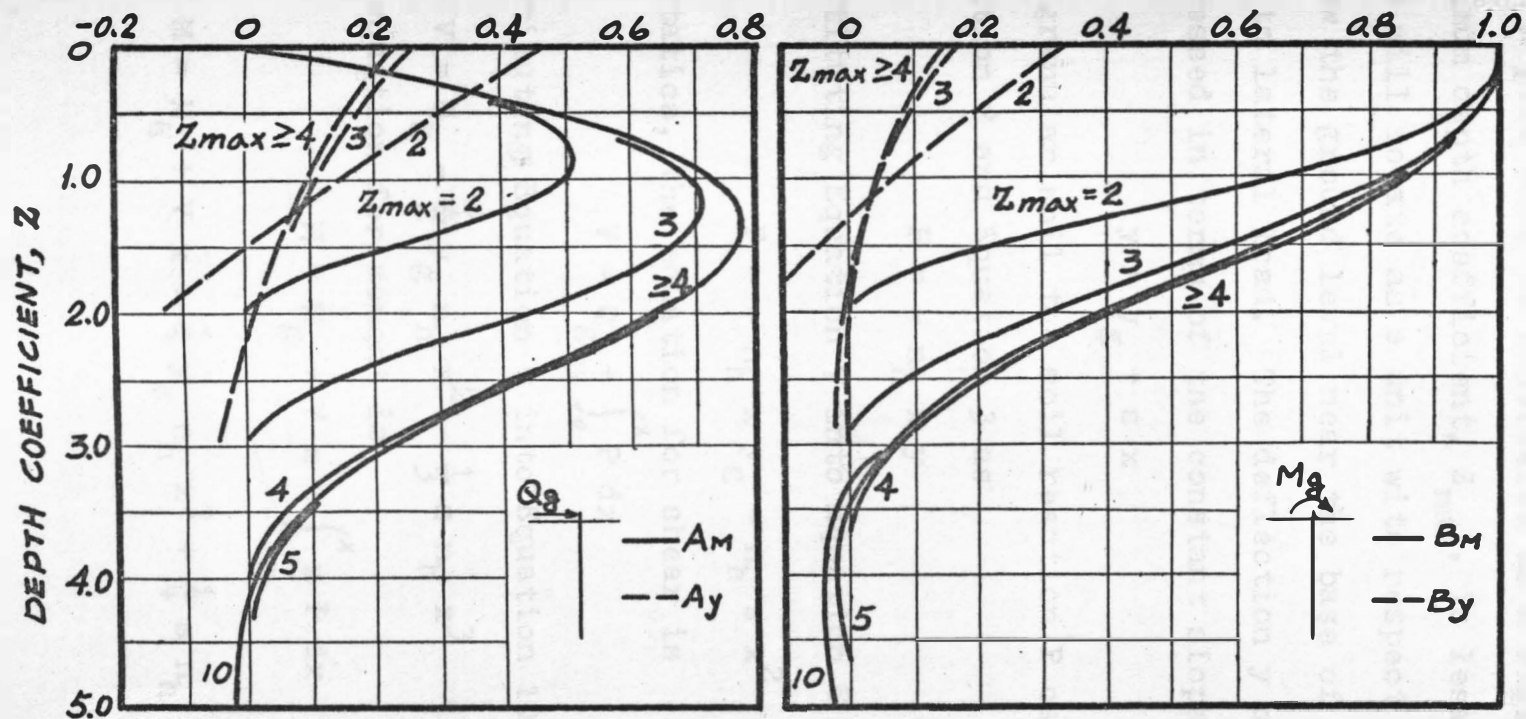
TABLE 1. NON-DIMENSIONAL COEFFICIENTS FOR $k = n_h \times (11)$

TERM	EQUATION
Depth coefficient	$z = \frac{x}{T}$
Maximum depth coefficient	$z_{\max} = \frac{L}{T}$
Relative stiffness factor	$T = \sqrt[5]{EI/n_h}$
Soil modulus function	$\Phi(z) = \frac{kT^4}{EI}$
Deflection coefficient due to Q_g alone	$A_y = \frac{y_A EI}{Q_g T^3}$
Deflection coefficient due to M_g alone	$B_y = \frac{y_B EI}{M_g T^2}$

TABLE 2. SOLUTIONS OF EQUATION 1 FOR $k = n_h \times (11)$

TERM	EQUATION
Deflection, y	$y = A_y \frac{Q_g T^3}{EI} + B_y \frac{M_g T^2}{EI}$
Slope, s	$s = A_s \frac{Q_g T^2}{EI} + B_s \frac{M_g T}{EI}$
Moment, M	$M = A_m Q_g T + B_m M_g$
Shear, V	$V = A_v Q_g + B_v M_g / T$
Soil reaction, P	$P = A_p Q_g / T + B_p M_g / T^2$

DEFLECTION AND MOMENT COEFFICIENTS, A_y AND A_m DEFLECTION AND MOMENT COEFFICIENTS, B_y AND B_m



(a) DEFLECTION AND MOMENT DUE TO LATERAL LOAD APPLIED AT GROUND SURFACE

(b) DEFLECTION AND MOMENT DUE TO MOMENT APPLIED AT GROUND SURFACE

FIGURE 3. INFLUENCE CURVES FOR DEFLECTION AND MOMENT OF FREE-HEADED PILE WHEN $k = n_h \times (11)$

Note: When determining the deflection coefficients A_y and B_y , multiply the values read from the graph by 10. No correction is necessary for the moment coefficients.

Rigid Pile Theory

A pile will be considered as a rigid one if its maximum depth coefficient, Z_{\max} , is less than 2. A rigid pile will rotate as a unit with respect to a point somewhere below the ground level near the base of the pile when subjected to lateral load. The deflection y of a rigid pile can be expressed in terms of the constant slope, s , of the pile as

$$y = y_g + s x \quad (7)$$

For granular soil the soil reaction P can be obtained from Equation 2 and Equation 3 as

$$P = - n_h x y \quad (8)$$

Substituting Equation 7 into Equation 8 gives

$$P = - n_h x y_g - n_h s x^2 \quad (9)$$

By statics, the equation for shear is

$$V = Q_g + \int_0^x P \, dx \quad (10)$$

Substituting Equation 9 into Equation 10,

$$V = Q_g - \frac{1}{2} y_g n_h x^2 - \frac{1}{3} s n_h x^3 \quad (11)$$

The equation for moment is

$$M = M_g + V x - \int_0^x x P \, dx \quad (12)$$

or

$$M = M_g + V x + \frac{1}{3} y_g n_h x^3 + \frac{1}{4} s n_h x^4 \quad (13)$$

The shear and moment are zero at the bottom of pile: at $x = L$, $V = 0$, and $M = 0$. Thus, Equations 14 and 15 may be written from Equations 11 and 13 so that y_g may be evaluated by simultaneous solution:

$$Q_g = \frac{1}{2} y_g n_h L^2 + \frac{1}{3} s n_h L^3 \quad (14)$$

$$M_g = \frac{1}{3} y_g n_h L^3 + \frac{1}{4} s n_h L^4 \quad (15)$$

(2) Broms' Combined Solutions

Deflections at Working Load

The lateral deflections at the ground surface, y_g , of a single pile in cohesionless soil can be expressed, at working loads, in terms of the dimensionless deflection y_g $(EI)^{3/5} (n_h)^{2/5} / QL$, and the dimensionless maximum depth coefficient, $Z_{max} = L/T$. The dimensionless lateral deflection at ground surface has been plotted in Figure 4 as a function of the dimensionless maximum depth coefficient Z_{max} . It can be seen from Figure 4 that a laterally loaded pile behaves as an infinitely stiff member when Z_{max} is less than about 2.0 and as an infinitely long member when Z_{max} exceeds about 4.0.

Ultimate Lateral Resistance

Broms assumed that the lateral earth pressure for cohesionless soil which develops at failure is equal to three times the passive Rankine earth pressure and is independent of the shape of the cross-sectional area of the

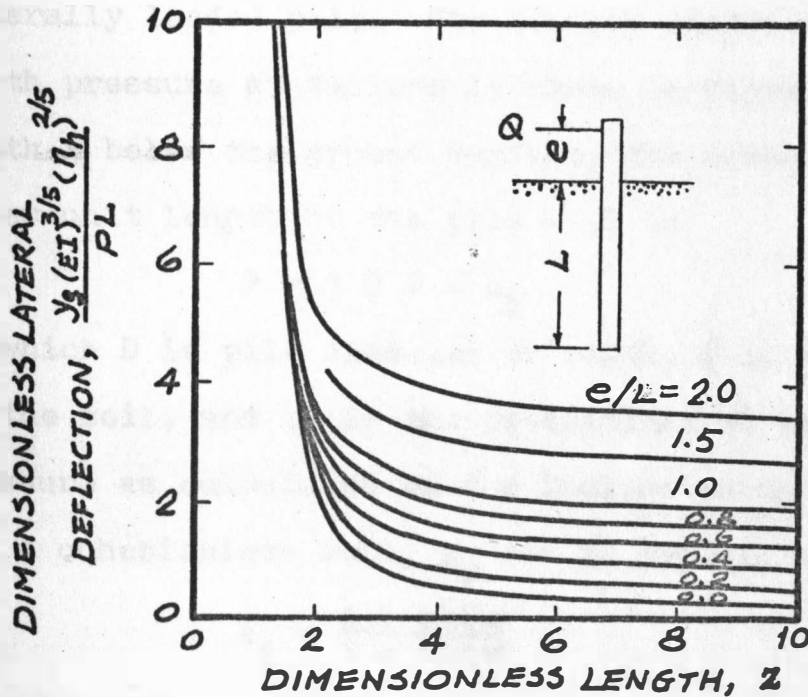


FIGURE 4. LATERAL DEFLECTIONS AT GROUND SURFACE FOR FREE-HEADED PILE (4)

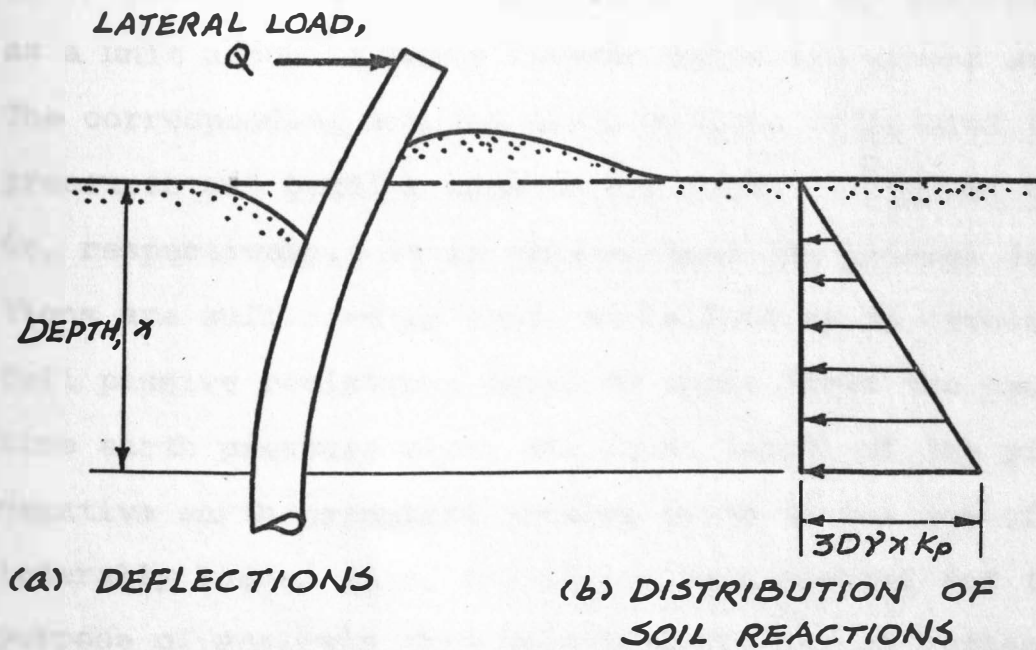


FIGURE 5. ASSUMED DISTRIBUTION OF SOIL REACTIONS

laterally loaded pile. The assumed distribution of lateral earth pressure at failure is shown in Figure 5. At the depth x below the ground surface, the assumed soil reaction P per unit length of the pile will be

$$P = 3 D \gamma x k_p \quad (16)$$

in which D is pile diameter or width, γ is the unit weight of the soil, and k_p is the coefficient of passive earth pressure as calculated by the Rankine earth pressure theory. For a cohesionless soil, k_p can be calculated from

$$k_p = \frac{1 + \sin\phi}{1 - \sin\phi} \quad (17)$$

in which ϕ is the angle of internal friction as determined from drained triaxial or direct shear test.

The mode of failure of a short free-headed pile is shown in Figure 6a. Failure occurs when the pile rotates as a unit around a point located below the ground surface. The corresponding assumed distributions of lateral earth pressures and bending moments are shown in Figures 6b and 6c, respectively. It is assumed that the lateral deflections are sufficiently large at failure as to develop the full passive resistance equal to three times the passive Rankine earth pressure along the total length of the pile. High negative earth pressures develop close to the toe of the laterally loaded pile, and it has been assumed for the purpose of analysis that this pressure can be replaced by

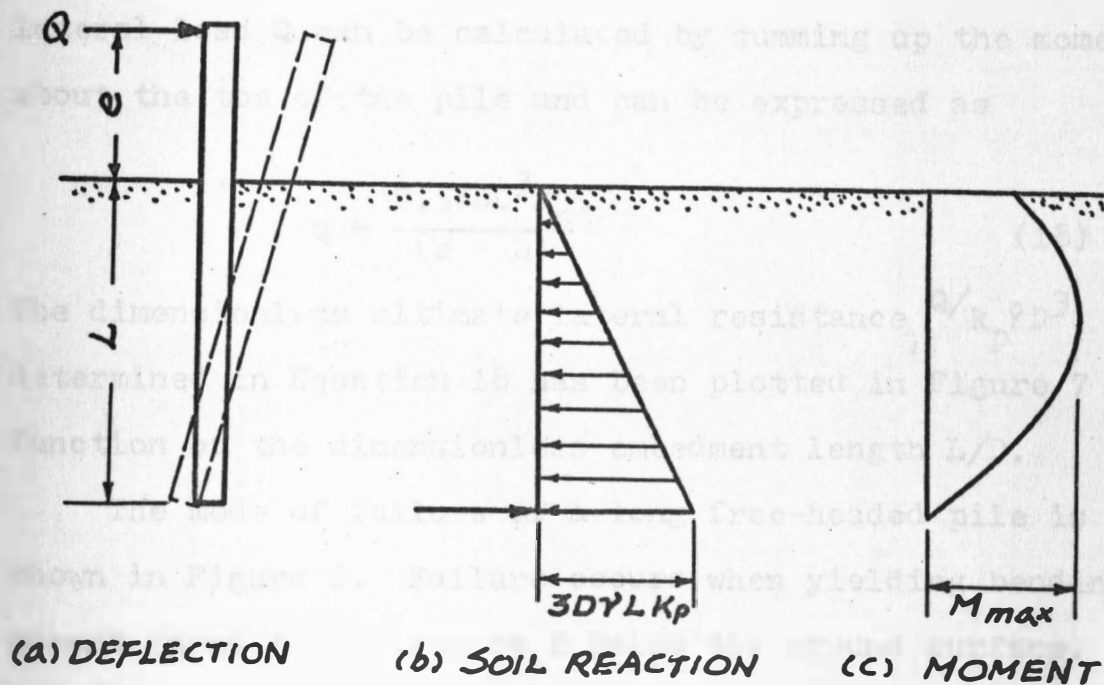


FIGURE 6. SHORT FREE-HEADED PILES DISTRIBUTION OF DEFLECTION, SOIL REACTION AND MOMENT

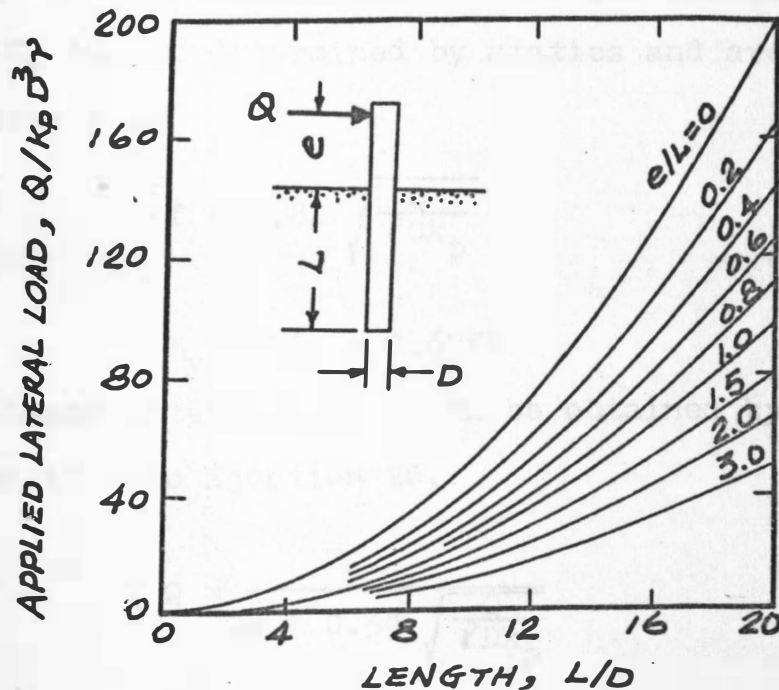


FIGURE 7. ULTIMATE LATERAL RESISTANCE OF SHORT FREE-HEADED PILES (4)

a concentrated load as shown in Figure 6b. The ultimate lateral load Q can be calculated by summing up the moments about the toe of the pile and can be expressed as

$$Q = \frac{0.5 \gamma D L^3 k_p}{(e + L)} \quad (18)$$

The dimensionless ultimate lateral resistance $Q/k_p \gamma D^3$ determined in Equation 18 has been plotted in Figure 7 as a function of the dimensionless embedment length L/D .

The mode of failure of a long free-headed pile is shown in Figure 8. Failure occurs when yielding bending moment forms at a distance f below the ground surface. It is assumed that the passive lateral earth pressure develops from the ground surface down to the location of the yielding bending moment. The distance f and the yielding bending moment M_y can be determined by statics and are expressed respectively as

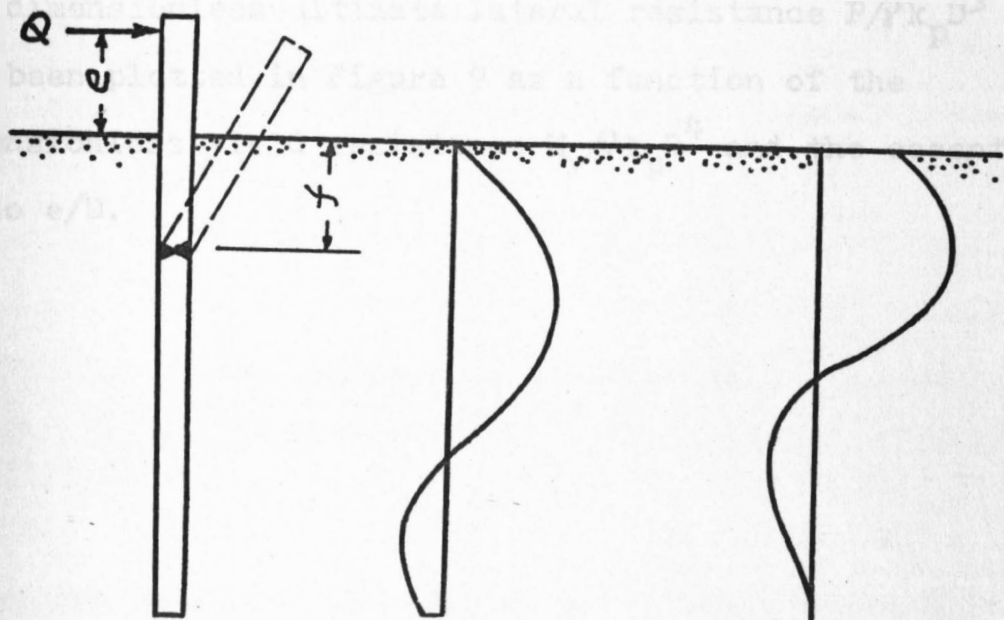
$$f = 0.82 \sqrt{\frac{Q}{\gamma D k_p}} \quad (19)$$

and

$$M_y = Q(e + 0.67f) \quad (20)$$

The ultimate lateral load Q can be obtained by substituting Equation 19 into Equation 20.

$$Q = \frac{M_y}{e + 0.54 \sqrt{\frac{Q}{\gamma D k_p}}} \quad (21)$$



(a) DEFLECTION (b) SOIL REACTIONS (c) BENDING MOMENT

FIGURE 8. LONG FREE-HEADED PILES DISTRIBUTION OF DEFLECTION, SOIL REACTIONS AND MOMENT

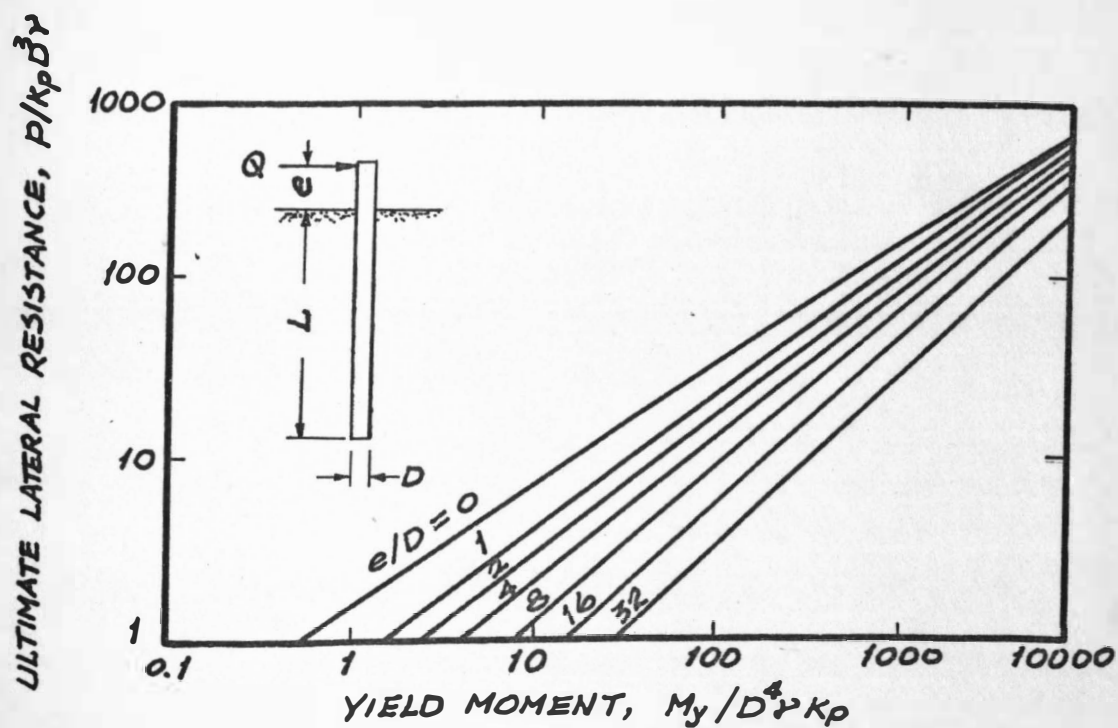


FIGURE 9. ULTIMATE LATERAL RESISTANCE OF LONG FREE-HEADED PILES (4)

The dimensionless ultimate lateral resistance $P/\gamma k_p D^3$ has been plotted in Figure 9 as a function of the dimensionless yield resistance $M_y/\gamma k_p D^4$ and the eccentricity ratio e/D .

EXPERIMENTAL INVESTIGATION

Loading tests to determine ultimate lateral loads were performed on twenty-three model piles. The model piles consisted of steel specimens having tubular, rectangular, or circular cross-sections. Table 3 lists the various physical properties of the test specimens.

Preparation of Soil

Dry sand passing through No. 4 sieve was used throughout the tests. Various properties pertaining to the sand soil are listed in Appendix B. The first series of tests were performed in a loose state of the sand soil; the second series of tests, in a medium dense state of the sand soil.

The container was a wood box with dimensions of 23-inch square cross section and 33-inch depth. Relative densities for loose sand, and medium dense sand were determined. Soil was then dumped in the box and vibrated until the required relative density was obtained.

Subgrade Modulus

The subgrade modulus of the sand soil used for the test was assumed to increase directly proportional to the depth below the ground surface, i.e., $k = n_h x$. An integral part of the analytical considerations for determining the load capacity of laterally loaded pile is the n_h value of

TABLE 3. PHYSICAL PROPERTIES OF MODEL PILE SPECIMENS

Specimen	Outside diameter in inches	Inside diameter in inches	I in ⁴ inches	E in pounds per inch ²	EI in pound-inches ²
3/8-inch steel bar	0.375	- -	0.000972	30×10^6	29,160
1/4-inch steel pipe	0.540	0.364	0.003310	30×10^6	99,300
3/8-inch steel bar	0.375 (width)	- -	0.001468	30×10^6	44,040
9/16-inch steel bar	0.563	- -	0.004920	30×10^6	147,600
1/2-inch steel pipe	0.840	0.622	0.017100	30×10^6	513,000

the particular soil. Before the predicted lateral load capacity could be determined, it was necessary to determine the n_h value.

Experimental Determination of n_h

The n_h value varied with relative density of the sand soil. Therefore, it was necessary to determine n_h for each test series. These determinations were completed by using the loading apparatus shown in Figure 10. The procedures employed were a modification of those suggested by Terzaghi for field test (1).

The test apparatus was a solid 7/8-inch square, 42-inch long steel bar embedded down to the total depth of the soil. The bottom end was restrained in a ball-and-socket arrangement and a load, Q , was applied to the upper end of the bar.

When a lateral load was applied to the top of the bar, a resisting pressure developed in the soil. Figure 11 shows the anticipated soil reaction from a lateral load for granular soil. The deflection at the ground surface of the bar, y_g , was measured for each load, Q . Summing up the moments about the pivot leads to the following equation:

$$n_h = \frac{12(L + e)}{L^3} \frac{Q}{y_g} \quad (28)$$

For the first test series, the loose sand acted almost elastically for small loading as shown in Figure 12.

Therefore, an n_h value of 6.72 pounds per cubic inch based

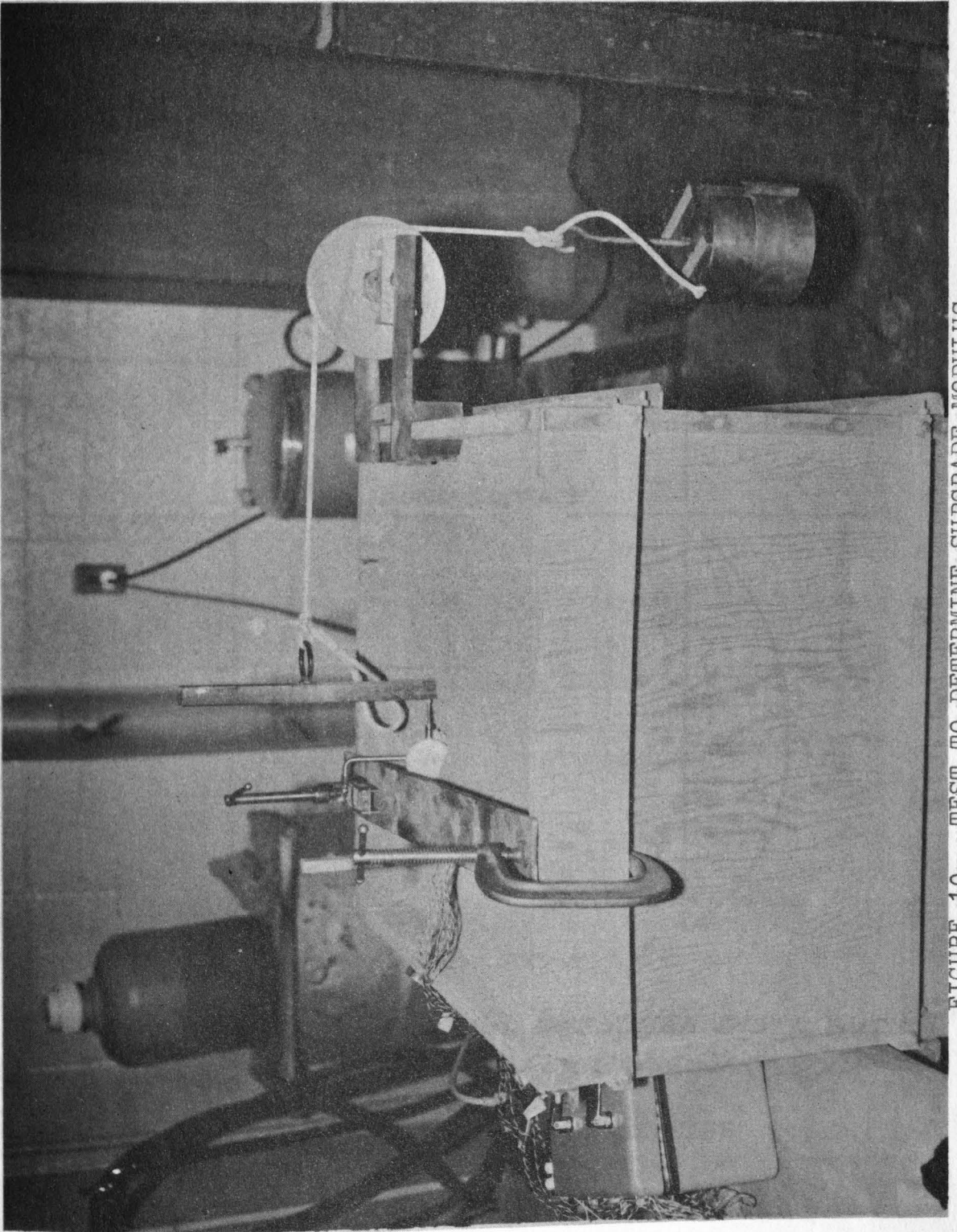
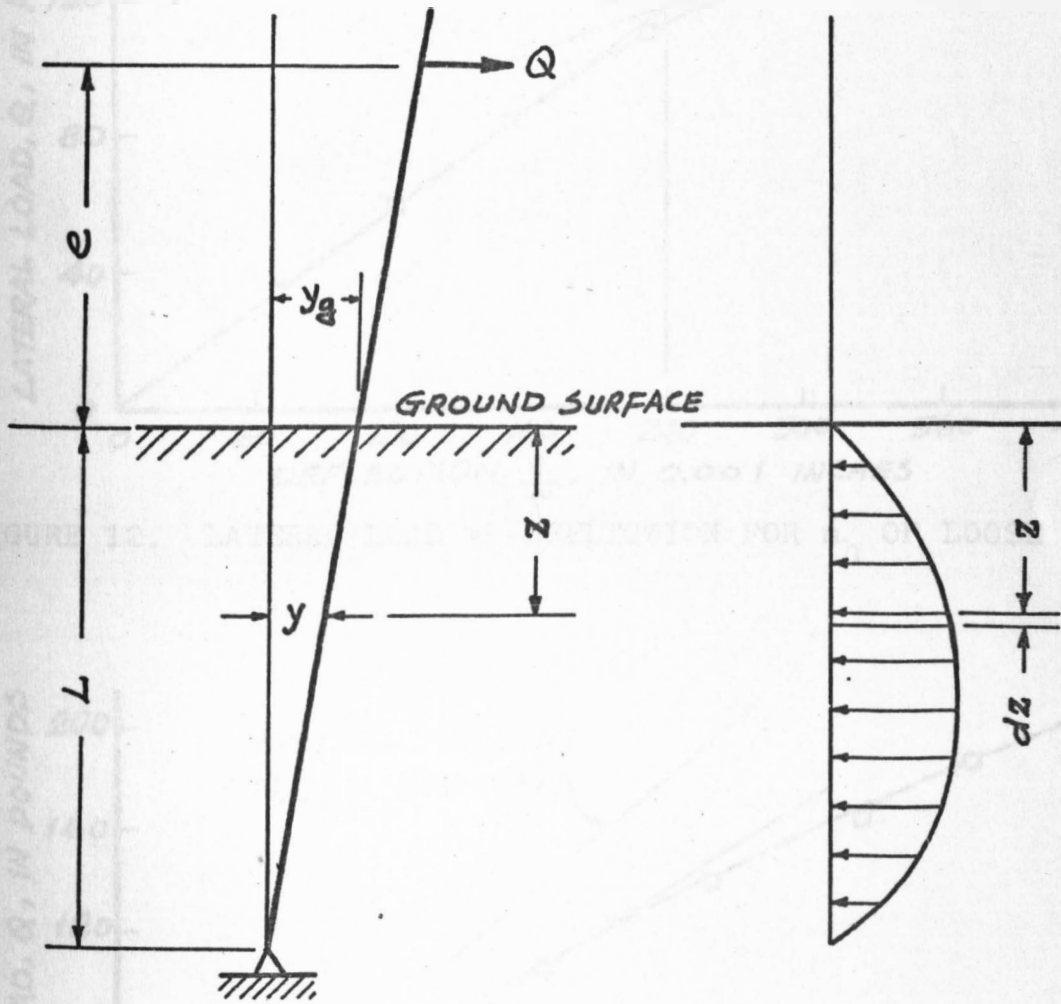


FIGURE 10. TEST TO DETERMINE SUBGRADE MODULUS



(a) DIMENSIONS

(b) PRESSURE DISTRIBUTION
FOR GRANULAR SOIL

FIGURE 11. DETERMINATION OF SUBGRADE MODULUS

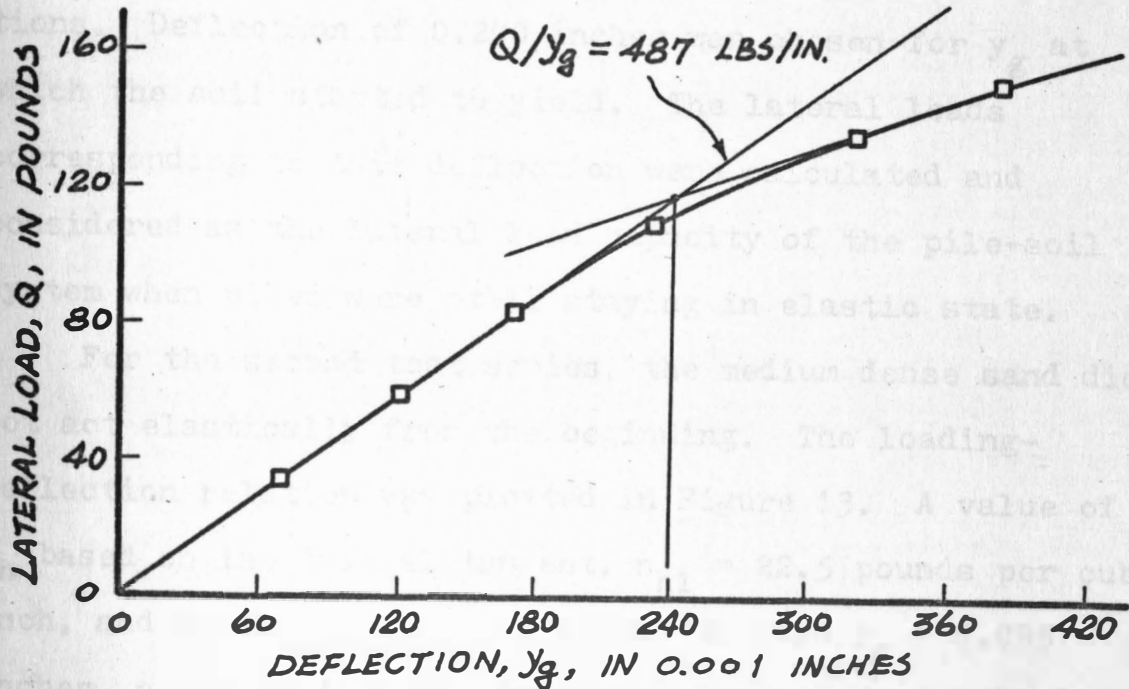


FIGURE 12. LATERAL LOAD vs DEFLECTION FOR n_h OF LOOSE SAND

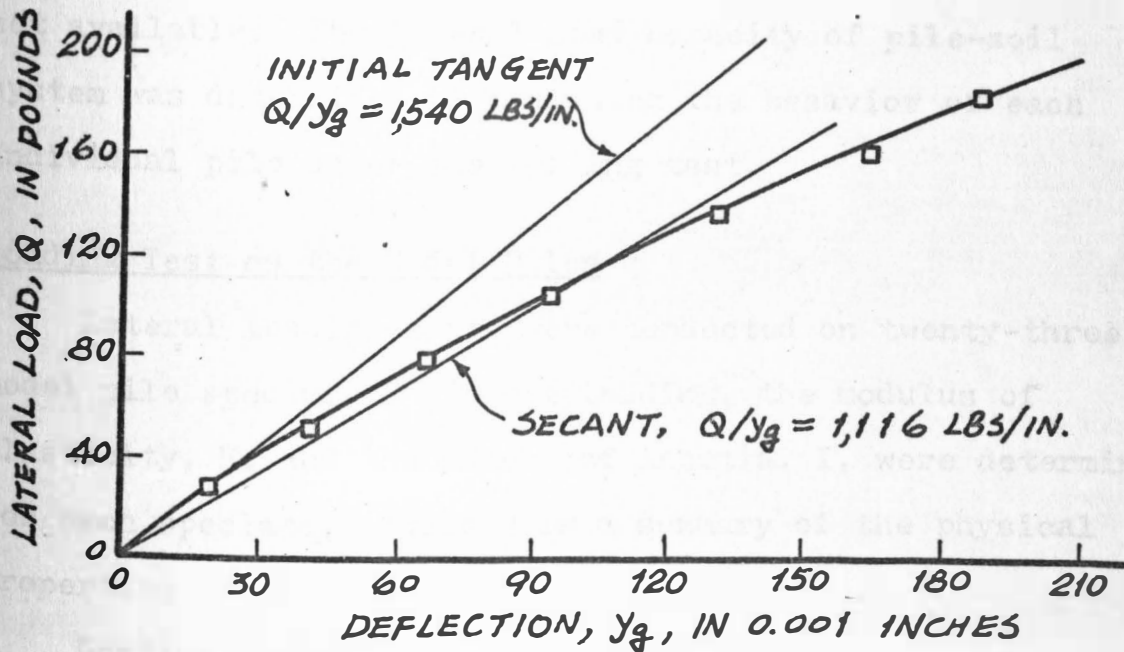


FIGURE 13. LATERAL LOAD vs DEFLECTION FOR n_h OF MEDIUM DENSE SAND

on the initial tangent was used for analytical considerations. Deflection of 0.240 inches was chosen for y_g at which the soil started to yield. The lateral loads corresponding to this deflection were calculated and considered as the lateral load capacity of the pile-soil system when piles were still staying in elastic state.

For the second test series, the medium dense sand did not act elastically from the beginning. The loading-deflection relation was plotted in Figure 13. A value of n_h based on the initial tangent, $n_{h1} = 22.5$ pounds per cubic inch, and another based on a secant through $y_g = 0.095$ inches, $n_{h2} = 18.1$ pounds per cubic inches, were calculated. Both values were tried in analytical considerations. An apparent value of y_g at which the soil started to yield was not available. The lateral load capacity of pile-soil system was determined by examining the behavior of each individual pile under the loading test.

Loading Test on the Model Piles

Lateral loading tests were conducted on twenty-three model pile specimens. Before loading, the modulus of elasticity, E , and the moment of inertia, I , were determined for each specimen. Table 3 is a summary of the physical properties of pile specimens.

Loading Device

Figure 14 shows the setup of the loading device with a

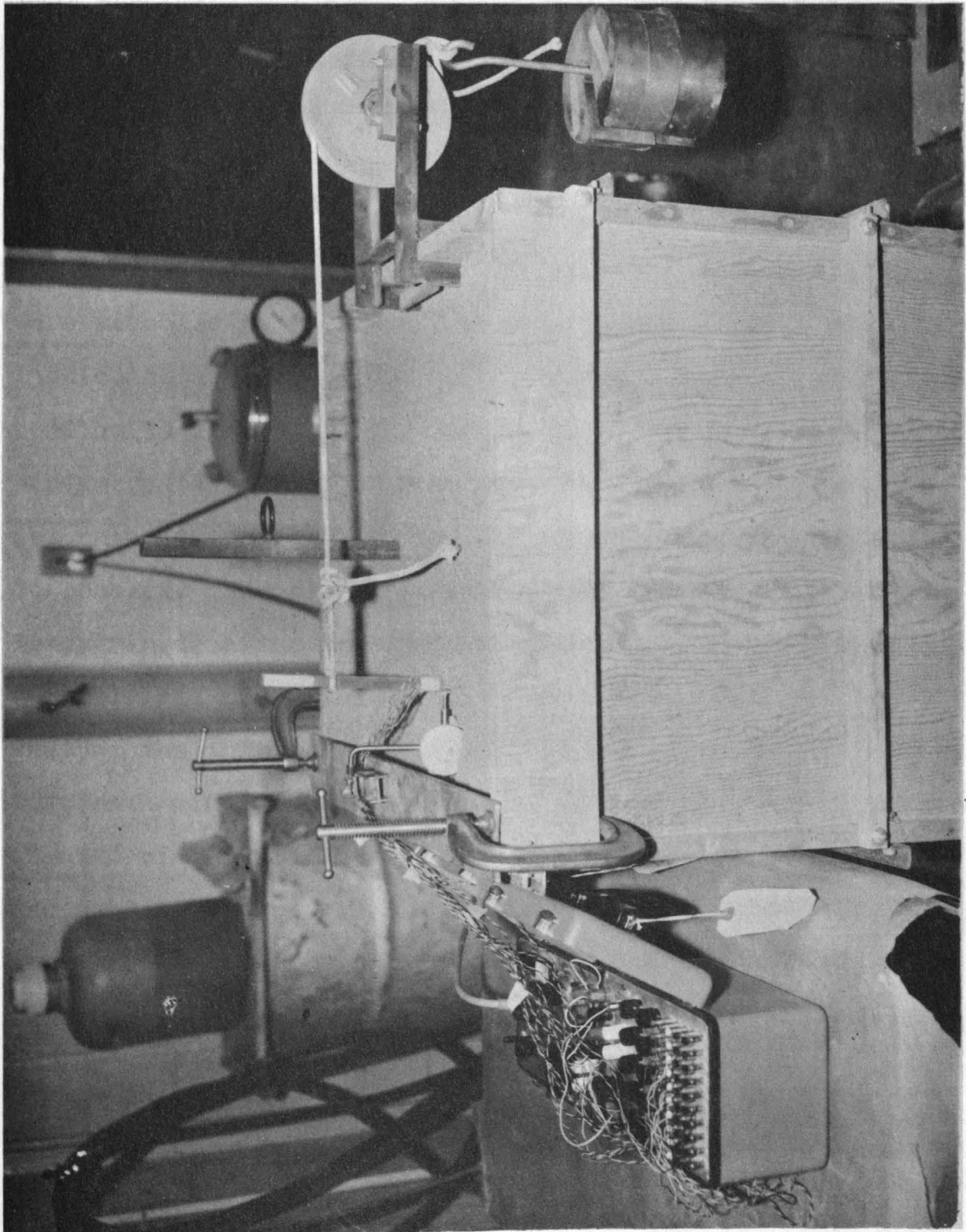


FIGURE 14. PILE LOADING APPARATUS

test specimen in place. The lateral load was applied somewhere above the ground surface by a cable, strung over a pulley, supporting a loading platform. Only static loading was used.

Lateral Deflection at Ground Surface

The lateral deflections of pile at ground surface, y_g , were measured by an Ames dial gage having a range of one inch calibrated to 0.001 inch. Readings were taken corresponding to each loading. A test on a 9/16-inch round steel bar embedded in medium dense sand was carried out to determine the effect of loading duration to pile lateral deflection. The deflection at ground surface, y_g , at the first minute after the application of each increment of lateral load was found to have taken place at least 90% of that at the thirtieth minute. The increase of y_g from the fifteenth minute to the thirtieth minute was found not more than 2% of the total at the thirtieth minute. Therefore, the sand soil used for tests was regarded as time independent and 20 minutes was chosen for the sustention of each increment of lateral loading.

Strain Gage Attachment

Two of the twenty-three model pile specimens were attached with electric resistance strain gages along the embedded portion for the measurement of flexural strains when subjected to lateral load. A bending moment curve

could therefore be plotted.

SR-4 Strain gages of paper-base type 16, manufactured by University Precision Measurement Company, Ann Arbor, Michigan, were used. The gage resistance is 120 ohms and gage factor 1.93. The gages were attached by using SR-4 cement and allowed to set at least twenty-four hours before a waterproof coating was applied to them. A switch and balance unit of Model SB-1 and a digital strain indicator of model p-350 of Budd Company, Phoenixville, Pennsylvania, were used for recording the flexural strain.

OBSERVED PERFORMANCE

Figures 15 through 20 show the relation of lateral load, Q , versus deflection at ground surface, y_g , for 3/8-inch round steel bars of various embedment lengths surrounded by loose sand. A critical deflection of $y_g = 0.240$ inches was chosen for the loose sand in the test as shown in Figure 12, and the corresponding lateral load was considered as the lateral resistance of the pile-soil system. Table 4 summarizes the test results of lateral resistance in comparison of the theoretical ones by using Matlock and Reese's generalized solutions. The experimental lateral resistances are found always to be greater than the computed values; that is, the analytical approach tends to be conservative. Deviations of no more than 20% were obtained for Z_{\max} from 2.90 up to 5.85. But greater deviations were found as Z_{\max} less than 2, thus showing excessive conservativeness for the rigid-pile theory of Matlock and Reese's generalized solutions. By interpolation, experimental lateral resistance $Q = 15.33$ pounds was obtained for $Z_{\max} = 4.0$. Comparing the lateral resistance corresponding to $Z_{\max} = 5.85$ with that of $Z_{\max} = 4$, an increase of only 8.05% was noted. Therefore, $Z_{\max} \geq 4$ is considered as a reasonable criterion for an infinitely long pile, although a value of 5 is more suitable. For the model pile with $Z_{\max} = 1.97$, computed results by using both elastic pile theory and rigid

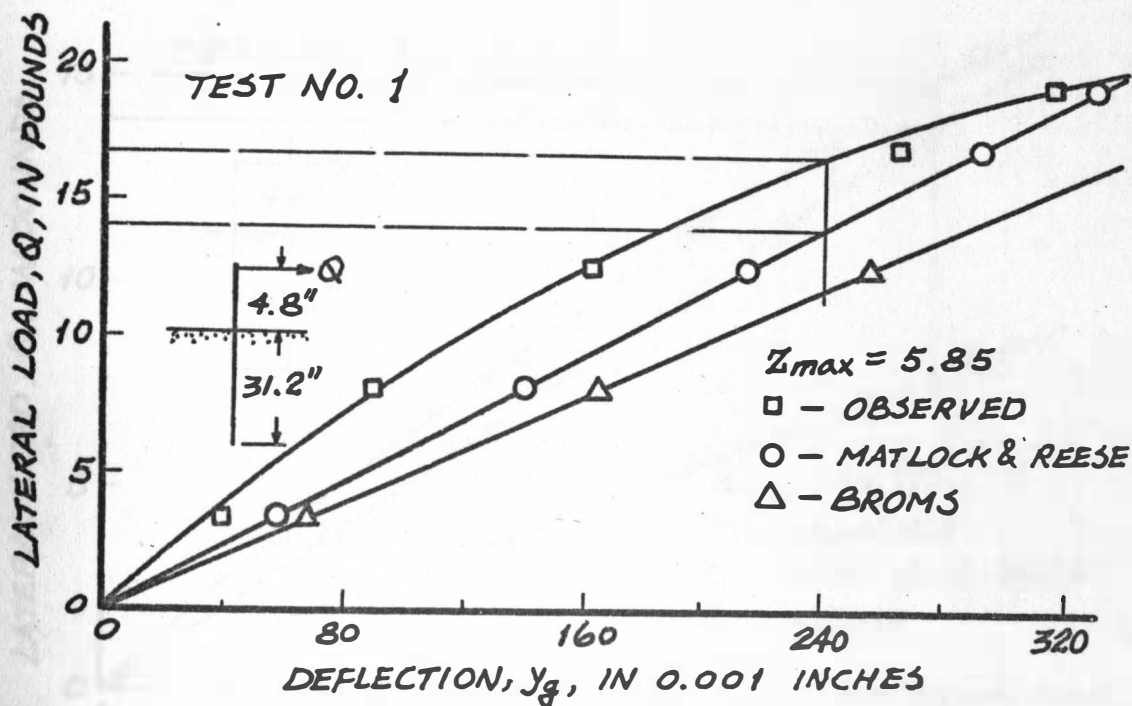


FIGURE 15. LATERAL LOAD vs DEFLECTION FOR 3/8-INCH ROUND STEEL BAR EMBEDDED IN LOOSE SAND

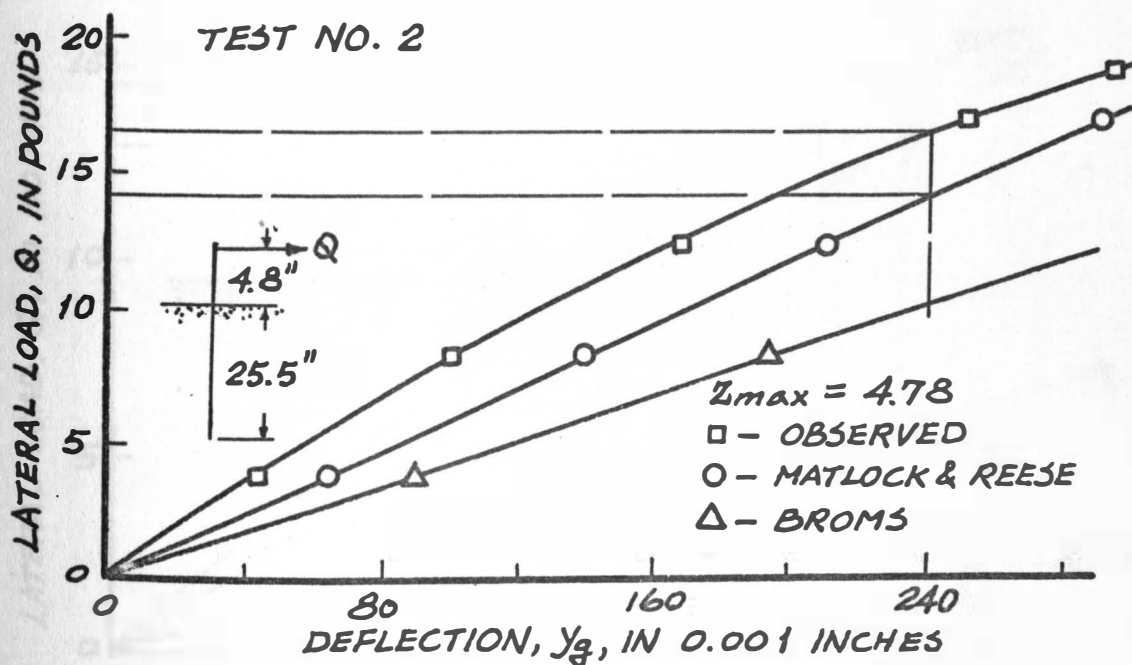


FIGURE 16. LATERAL LOAD vs DEFLECTION FOR 3/8-INCH ROUND STEEL BAR EMBEDDED IN LOOSE SAND

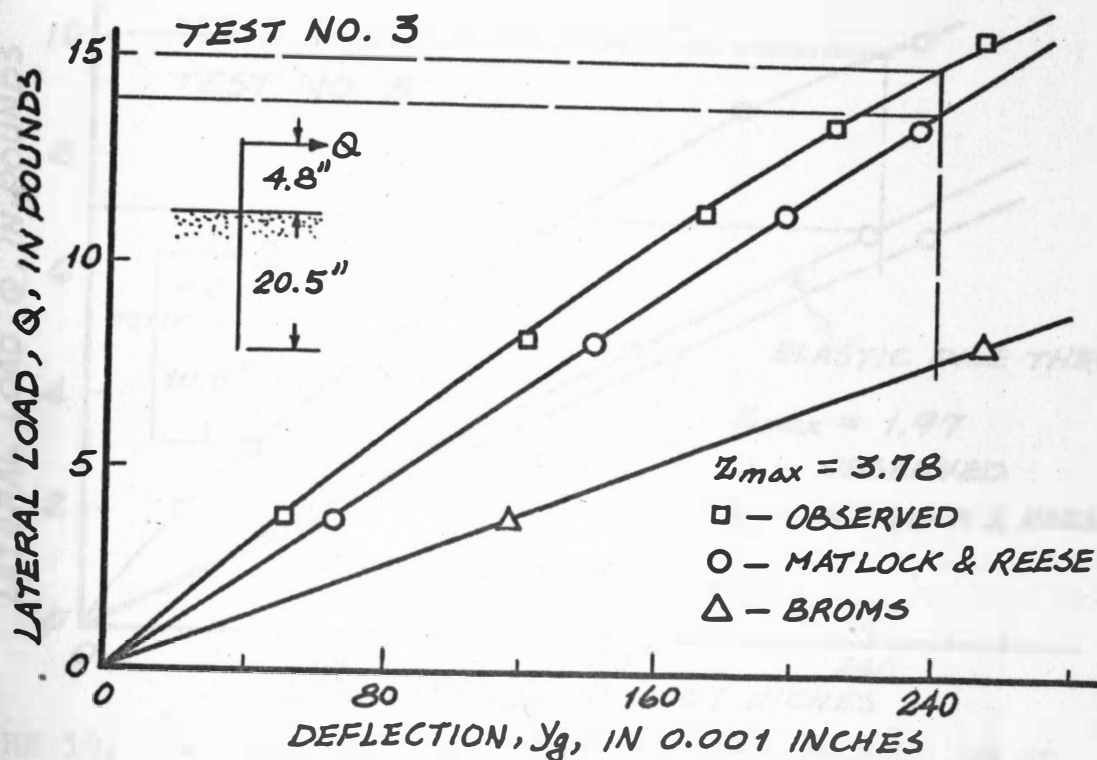


FIGURE 17. LATERAL LOAD vs DEFLECTION FOR 3/8-INCH ROUND STEEL BAR EMBEDDED IN LOOSE SAND

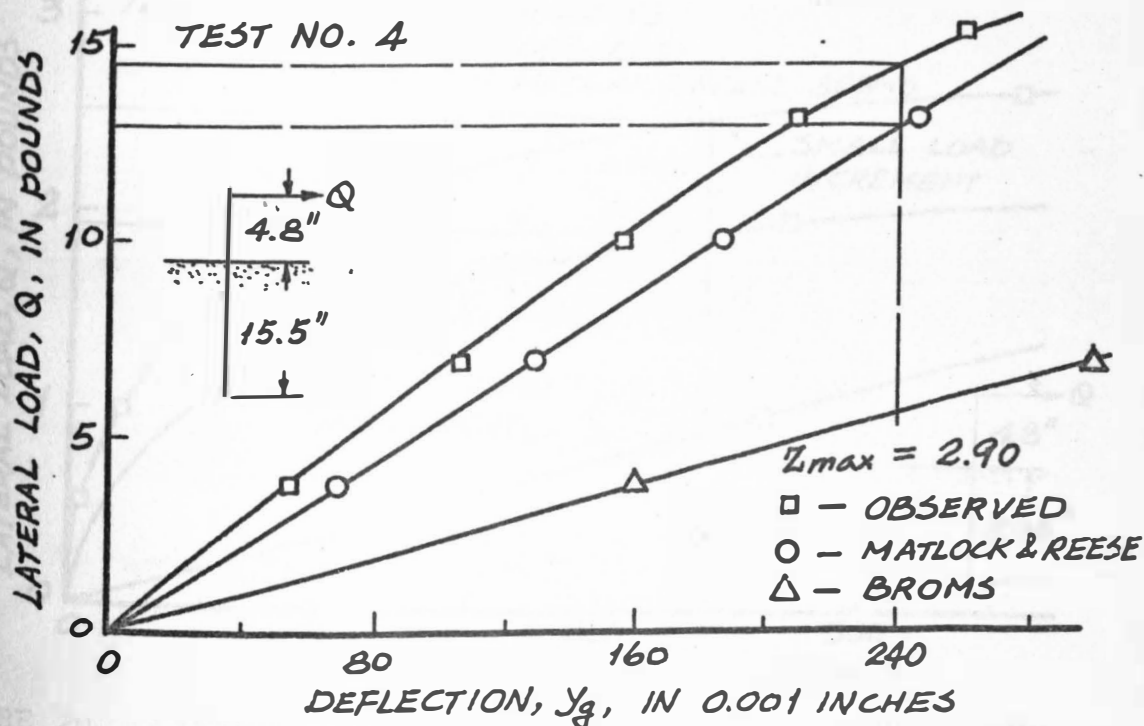


FIGURE 18. LATERAL LOAD vs DEFLECTION FOR 3/8-INCH ROUND STEEL BAR EMBEDDED IN LOOSE SAND

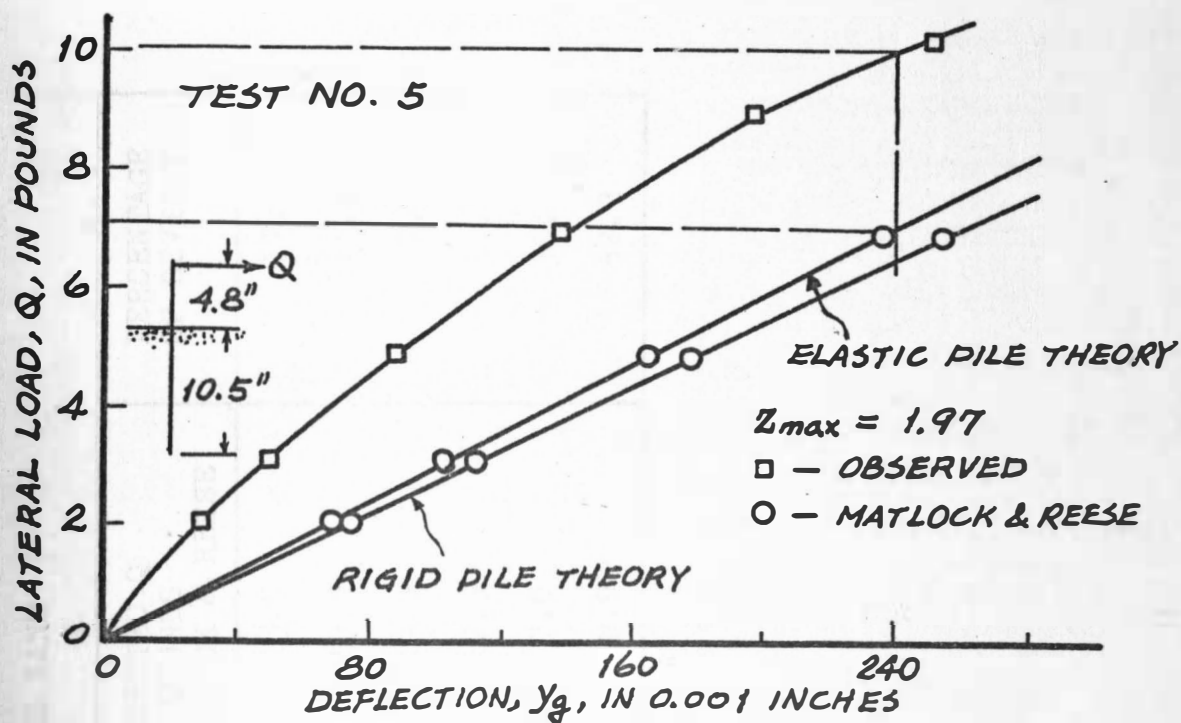


FIGURE 19. LATERAL LOAD vs DEFLECTION FOR 3/8-INCH ROUND STEEL BAR EMBEDDED IN LOOSE SAND

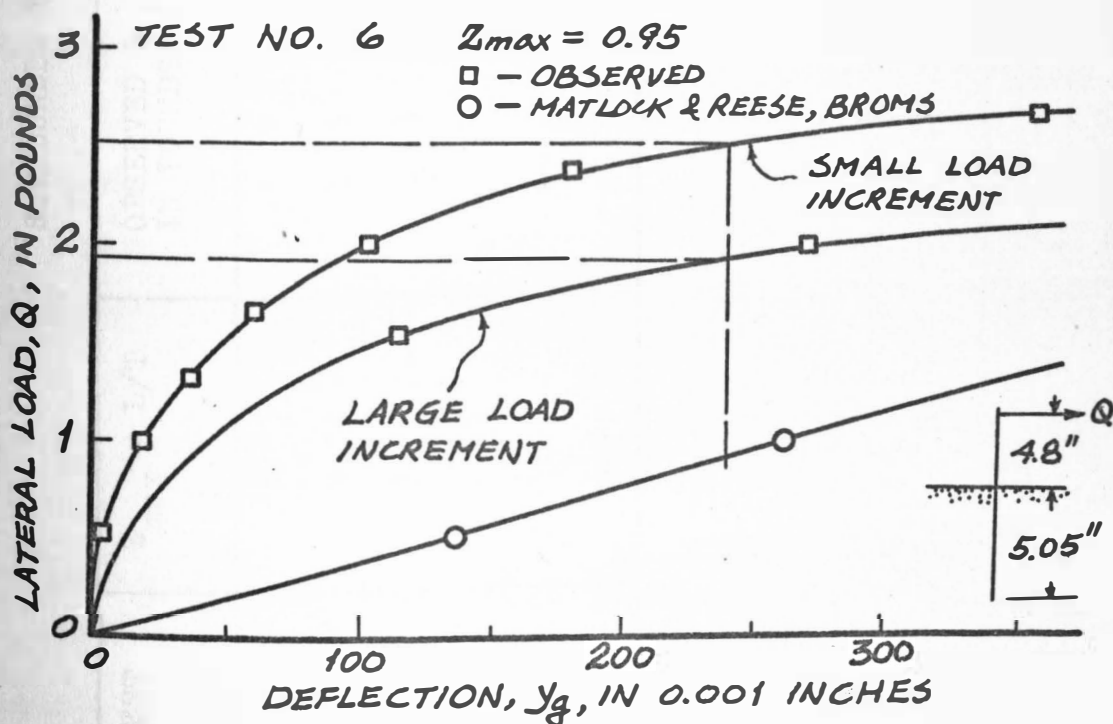


FIGURE 20. LATERAL LOAD vs DEFLECTION FOR 3/8-INCH ROUND STEEL BAR EMBEDDED IN LOOSE SAND

TABLE 4. LATERAL RESISTANCES, Q, FOR 3/8-INCH ROUND STEEL BARS
SURROUNDED BY LOOSE SAND

TEST NO.	$z_{\max} = L/T$	OBSERVED Q IN POUNDS	COMPUTED Q IN POUNDS MATLOCK & REESE	PERCENTAGE OF DEVIATION
1	5.85	16.7	13.9	17.7
2	4.78	16.5	13.9	15.8
3	3.78	15.0	13.9	7.3
4	2.90	14.4	12.9	10.4
5	1.97	10.1	7.0	30.7
6	0.95	1.93	0.92	52.3

pile theory of Matlock and Reese's generalized solutions are presented in Figure 19. The deviation between these two values was less than 5%. Figure 20 also shows the effect of loading increments on deflections for a very short pile. The large loading increment was found to create much greater deflections than the small one.

Theoretical lateral load and deflection relation of 3/8-inch round steel bars by using Broms' method are also presented in Figures 15 through 20. The allowable lateral loads corresponding to one-half of the critical deflection $y_g = 0.240$ inches were determined. A summary of these values are presented in Table 5. Those theoretical allowable lateral loads by using Broms method were found too conservative and will be uneconomical if used for designing. Deviations of from 42.1% up to 70.6% were obtained for the tests conducted.

Figures 21 through 25 show the relation of lateral load, Q , versus deflection at ground surface, y_g , for 1/4-inch steel tubes of various embedment lengths surrounded by medium dense sand. After studying every individual load-deflection curve, a critical deflection of $y_g = 0.200$ inches was chosen for the medium dense sand in test, and the corresponding lateral load was considered as the lateral resistance of the pile-soil system. The propriety of choosing 0.200 inches as the critical deflection of y_g for

TABLE 5. LATERAL LOADS, Q , CORRESPONDING TO $y_g = 0.12Q$ INCHES

FOR 3/8-INCH ROUND STEEL BARS SURROUNDED BY

LOOSE SAND

TEST NO.	OBSERVED Q IN POUNDS	MATLOCK AND REESE METHOD		BROMS METHOD	
		COMPUTED Q IN POUNDS	PERCENTAGE OF DEVIATION	COMPUTED Q IN POUNDS	PERCENTAGE OF DEVIATION
1	10.20	7.00	31.4	5.90	42.1
2	9.55	7.30	23.6	5.00	46.6
3	8.30	6.95	16.3	3.88	53.2
4	8.01	6.45	19.5	2.84	64.5
5	6.22	3.55	42.9	--	--
6	1.57	0.46	70.6	0.46	70.6

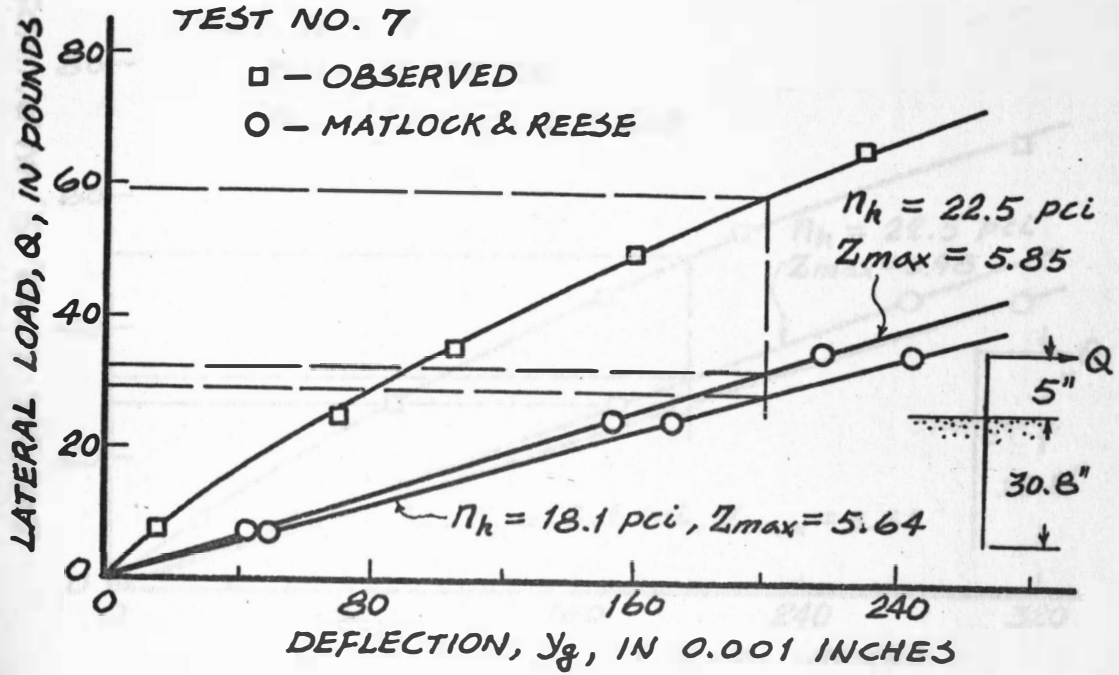


FIGURE 21. LATERAL LOAD vs DEFLECTION FOR 1/4-INCH STEEL TUBE EMBEDDED IN MEDIUM DENSE SAND

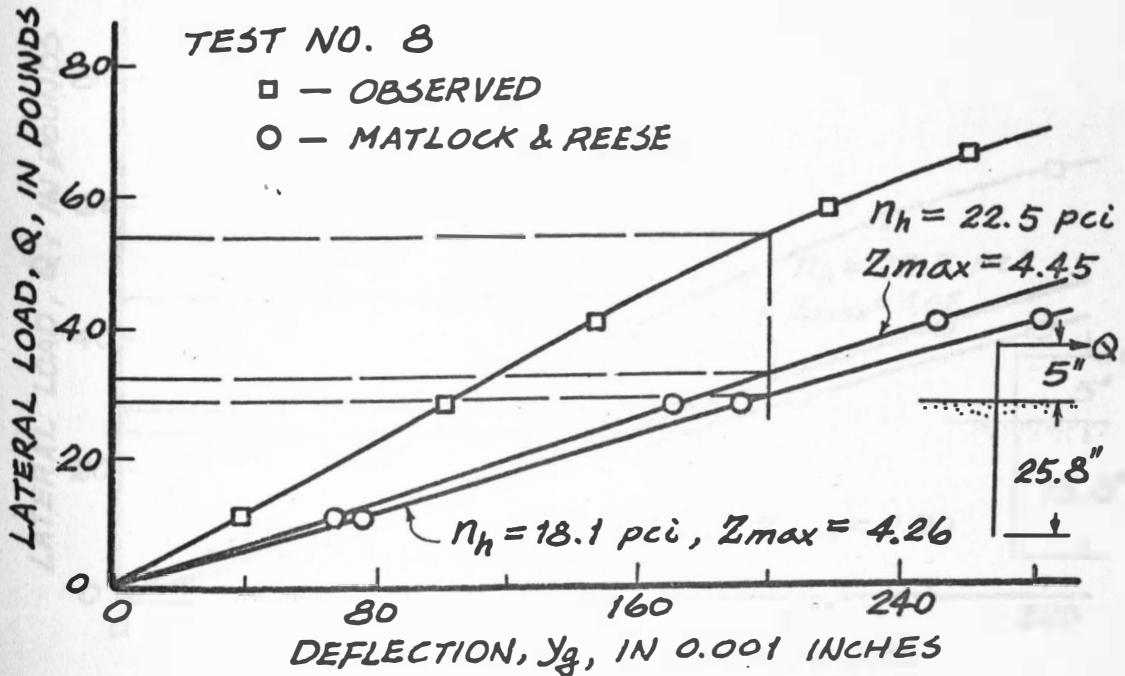


FIGURE 22. LATERAL LOAD vs DEFLECTION FOR 1/4-INCH STEEL TUBE EMBEDDED IN MEDIUM DENSE SAND

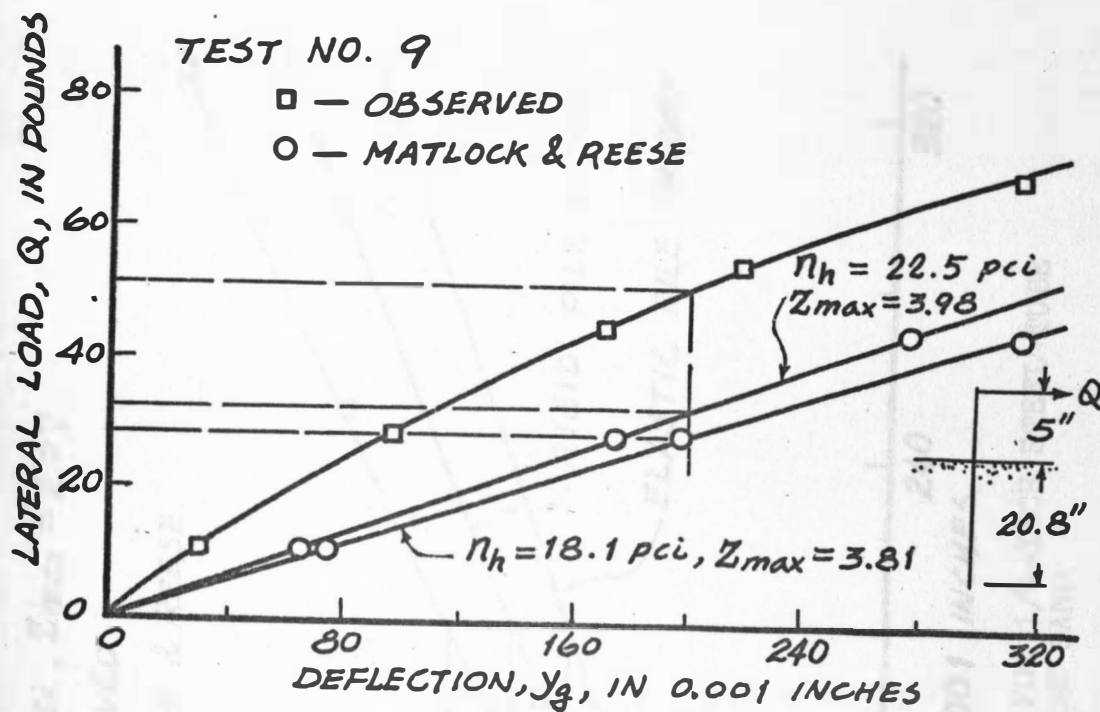


FIGURE 23. LATERAL LOAD vs DEFLECTION FOR 1/4-INCH STEEL TUBE EMBEDDED IN MEDIUM DENSE SAND

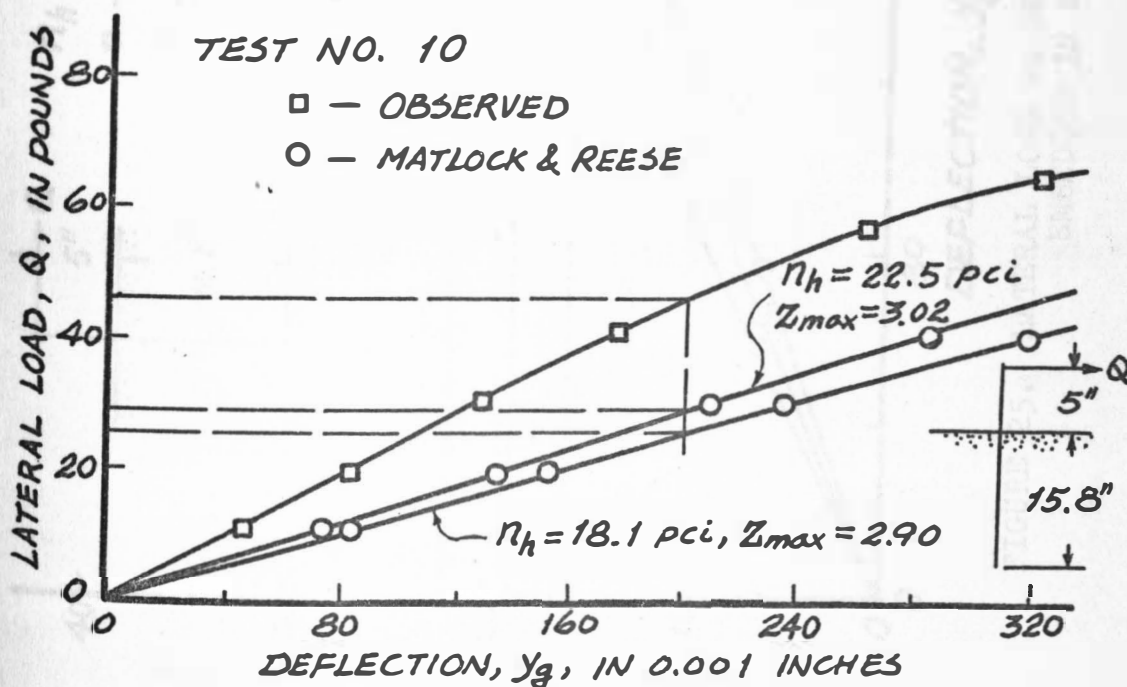


FIGURE 24. LATERAL LOAD vs DEFLECTION FOR 1/4-INCH STEEL TUBE EMBEDDED IN MEDIUM DENSE SAND

TEST NO. 11

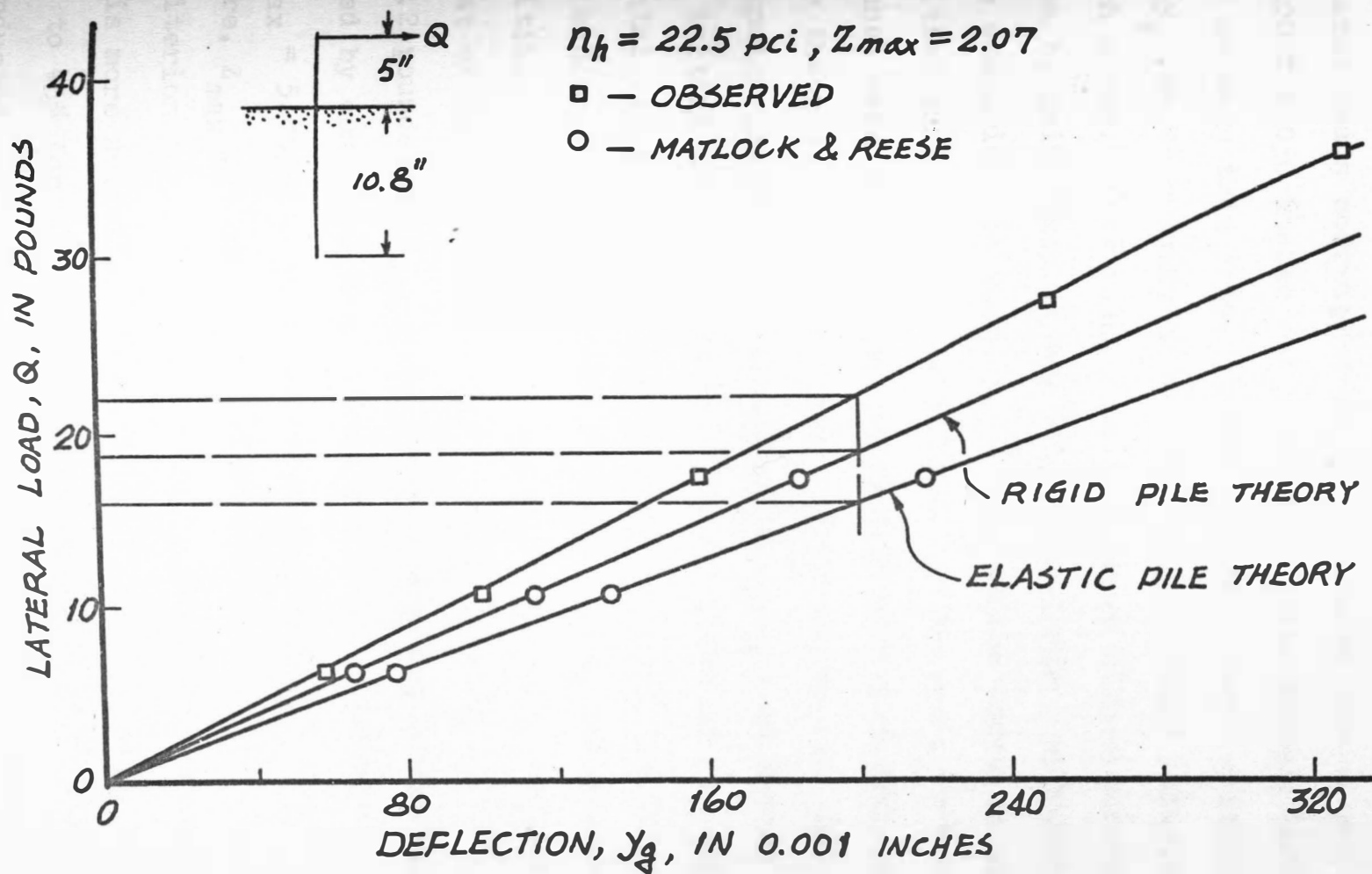


FIGURE 25. LATERAL LOAD vs DEFLECTION FOR 1/4-INCH STEEL TUBE EMBEDDED IN MEDIUM DENSE SAND

the medium dense sand was justified by comparing the lateral loads corresponding to $y_g = 0.200$ inches and $y_g = 0.200 \pm 0.050$ inches for each test. The maximum difference was no more than 3.5%. Therefore, the chosen critical value of y_g can be considered as reasonable without inducing too much error. Test results were compared with theoretical ones by using Matlock and Reese's analytical approach and are summarized in Table 6. Two n_h values based on an initial tangent and a secant passing through $y_g = 0.095$ inches were tried for the analytical computations. Again, the theoretical values showed conservativeness. The computed lateral resistances by using $n_h = 22.5$ pci based on initial tangent were found to be closer to the experimental results than those of using $n_h = 18.1$ pci based on an arbitrary chosen secant. Hence, the n_h value based on initial tangent was used for analytical computations in the rest of the study. The experimental lateral resistance is 51.2 pounds for $Z_{\max} = 4.0$. An increase of 13.5% was obtained by comparing the lateral resistance corresponding to $Z_{\max} = 5.85$ with that corresponding to $Z_{\max} = 4.0$. Therefore, $Z_{\max} \geq 4$ can be considered as fairly reasonable criterion for an infinitely long pile, although a value of 5 is more suitable. Deviations of 36.2% for $Z_{\max} = 3.02$ up to 45% for $Z_{\max} = 5.85$ were obtained for the test conducted. Deviation of 14.5% for the test specimen with $Z_{\max} = 2.07$ shows that the rigid pile theory of Matlock and

TABLE 6. LATERAL RESISTANCES, Q, FOR 1/4-INCH STEEL PIPES
EMBEDDED IN MEDIUM DENSE SAND

TEST NO.	OBSERVED Q IN POUNDS	$n_h = 22.5 \text{ LBS/INCH}^3$			$n_h = 18.1 \text{ LBS/INCH}^3$		
		Z_{\max}	COMPUTED Q IN POUNDS	PERCENTAGE OF DEVIATION	Z_{\max}	COMPUTED Q IN POUNDS	PERCENTAGE OF DEVIATION
7	59.2	5.85	32.5	45.0	5.64	29.0	49.9
8	54.0	4.45	32.5	39.8	4.26	29.0	46.3
9	51.2	3.98	32.5	37.6	3.81	29.0	44.3
10	46.3	3.02	29.0	36.2	2.90	26.0	42.8
11	24.2	2.07	18.8	14.5	--	--	--

Reese's generalized solutions is a good analytical approach for medium dense sand.

Figures 26 through 30 show the relation of lateral load, Q , versus deflection at ground surface, y_g , for 9/16-inch round steel bars of various embedment lengths surrounded by medium dense sand. Experimental lateral resistances were determined according to the critical deflection $y_g = 0.200$ inches, and are summarized in Table 7 in comparison with the theoretical values computed by using Matlock and Reese's generalized solutions. The analytical approach tends to be conservative. The experimental lateral resistance was 57.0 pounds for $Z_{\max} = 4.0$ by interpolation. An increase of 19.1% was noted by comparing the lateral resistance corresponding to $Z_{\max} = 5.31$ with that corresponding to $Z_{\max} = 4.0$. Therefore, $Z_{\max} \geq 4$ can still be considered as the criterion of an infinitely long pile, although the result is not too good, and a value of 5 for Z_{\max} would be more suitable. Deviations between the experimental lateral resistance and theoretical ones varied from around 30% to 40% for Z_{\max} values ranging from 2.72 to 5.31. Deviation of only 12.8% was noted for $Z_{\max} = 1.86$ showing fairly good agreement between the rigid pile theory and the actual behavior of a short pile.

Theoretical lateral load and deflection relation of 9/16-inch round steel bars by using Broms' method are also

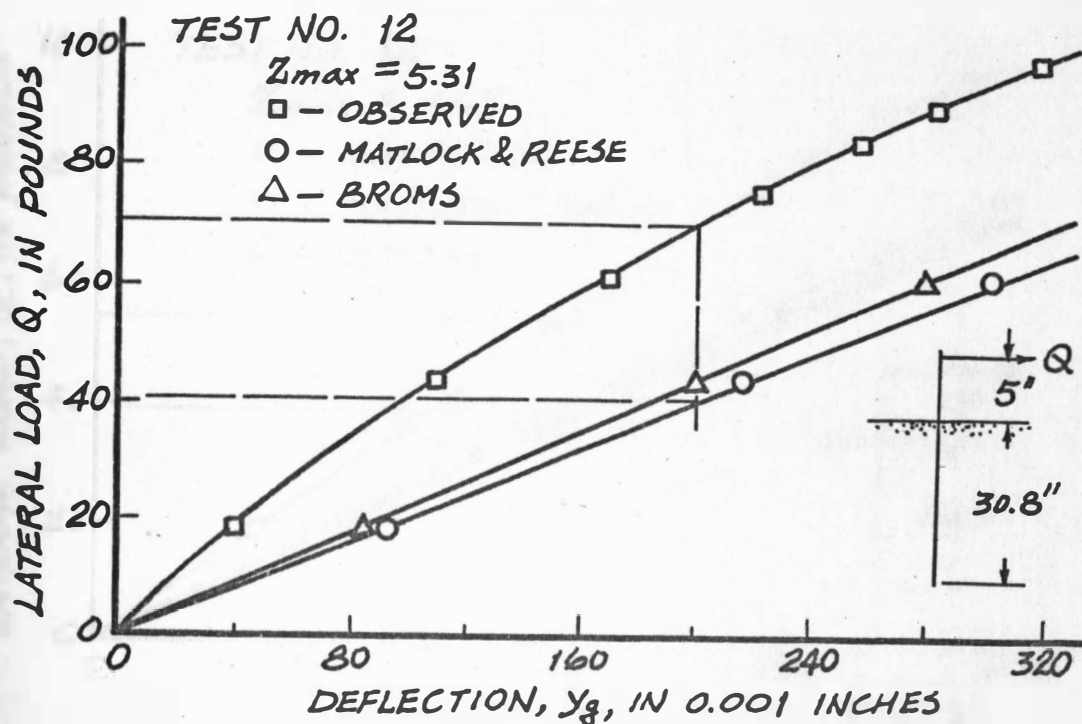


FIGURE 26. LATERAL LOAD vs DEFLECTION FOR 9/16-INCH STEEL BAR EMBEDDED IN MEDIUM DENSE SAND

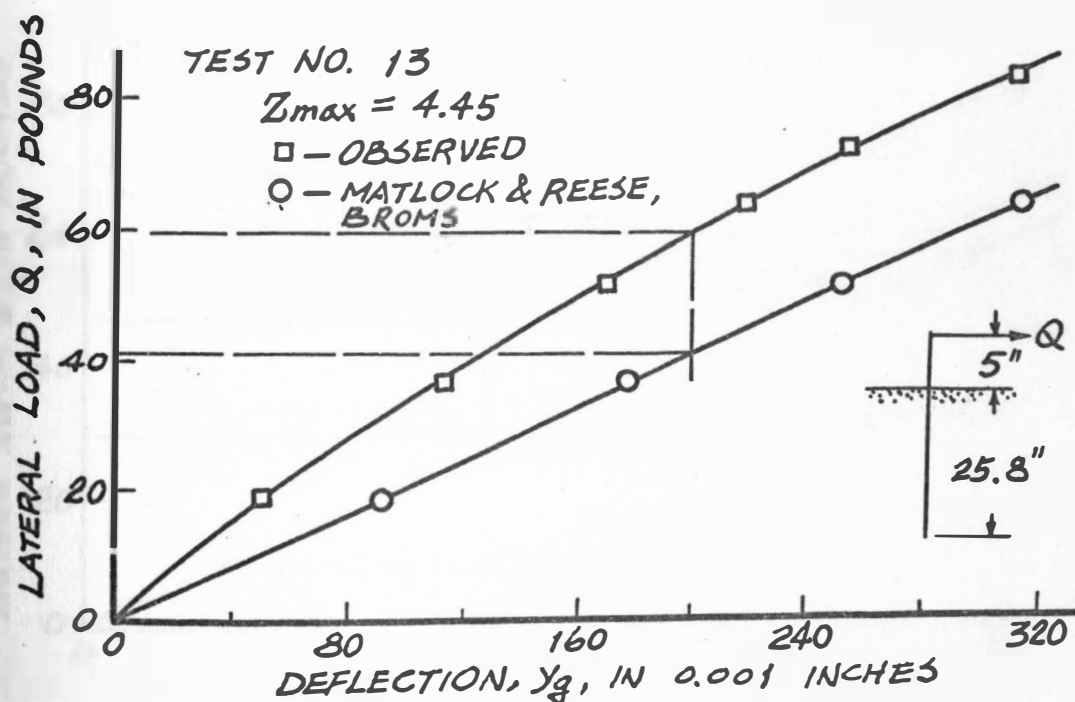


FIGURE 27. LATERAL LOAD vs DEFLECTION FOR 9/16-INCH STEEL BAR EMBEDDED IN MEDIUM DENSE SAND

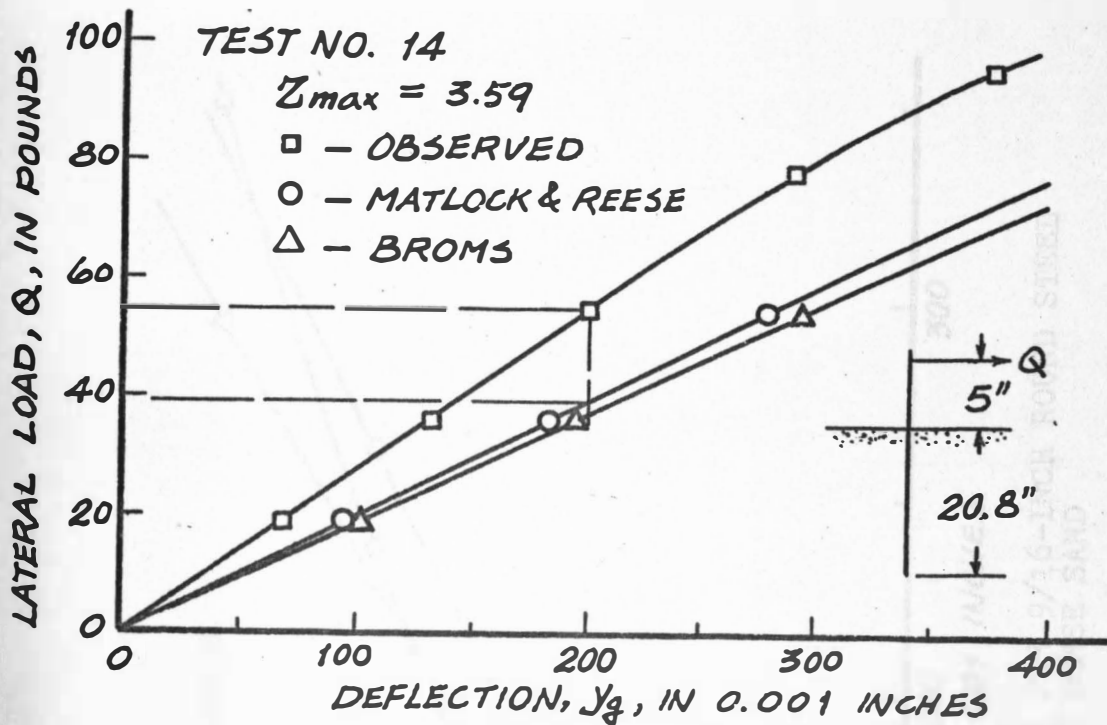


FIGURE 28. LATERAL LOAD vs DEFLECTION FOR 9/16-INCH ROUND STEEL BAR EMBEDDED IN MEDIUM DENSE SAND

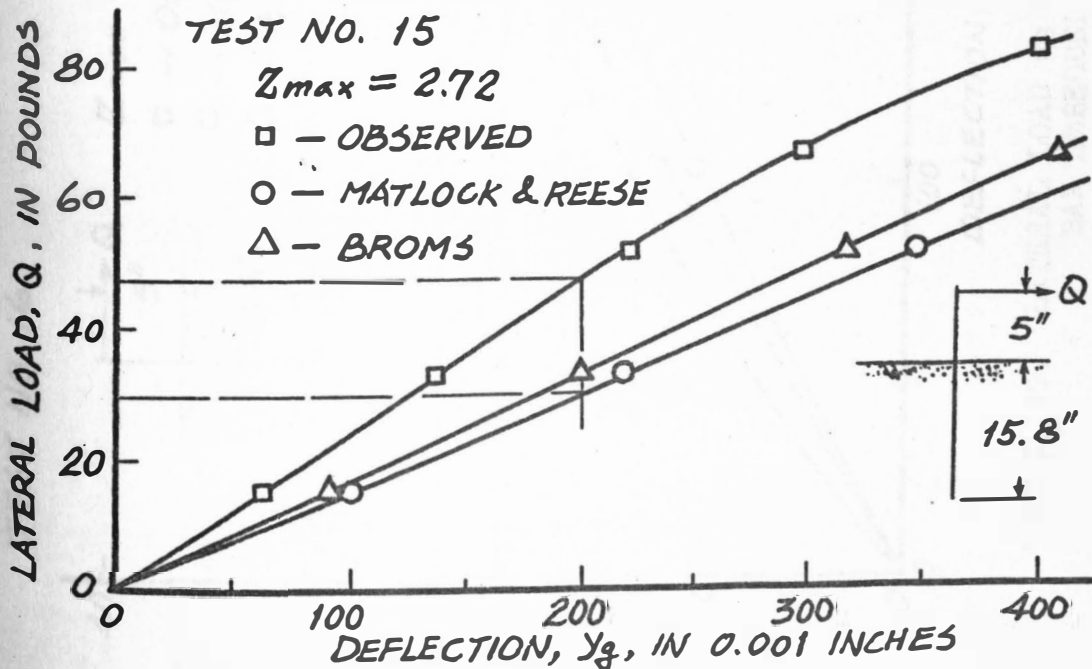


FIGURE 29. LATERAL LOAD vs DEFLECTION FOR 9/16-INCH ROUND STEEL BAR EMBEDDED IN MEDIUM DENSE SAND

TEST NO. 16

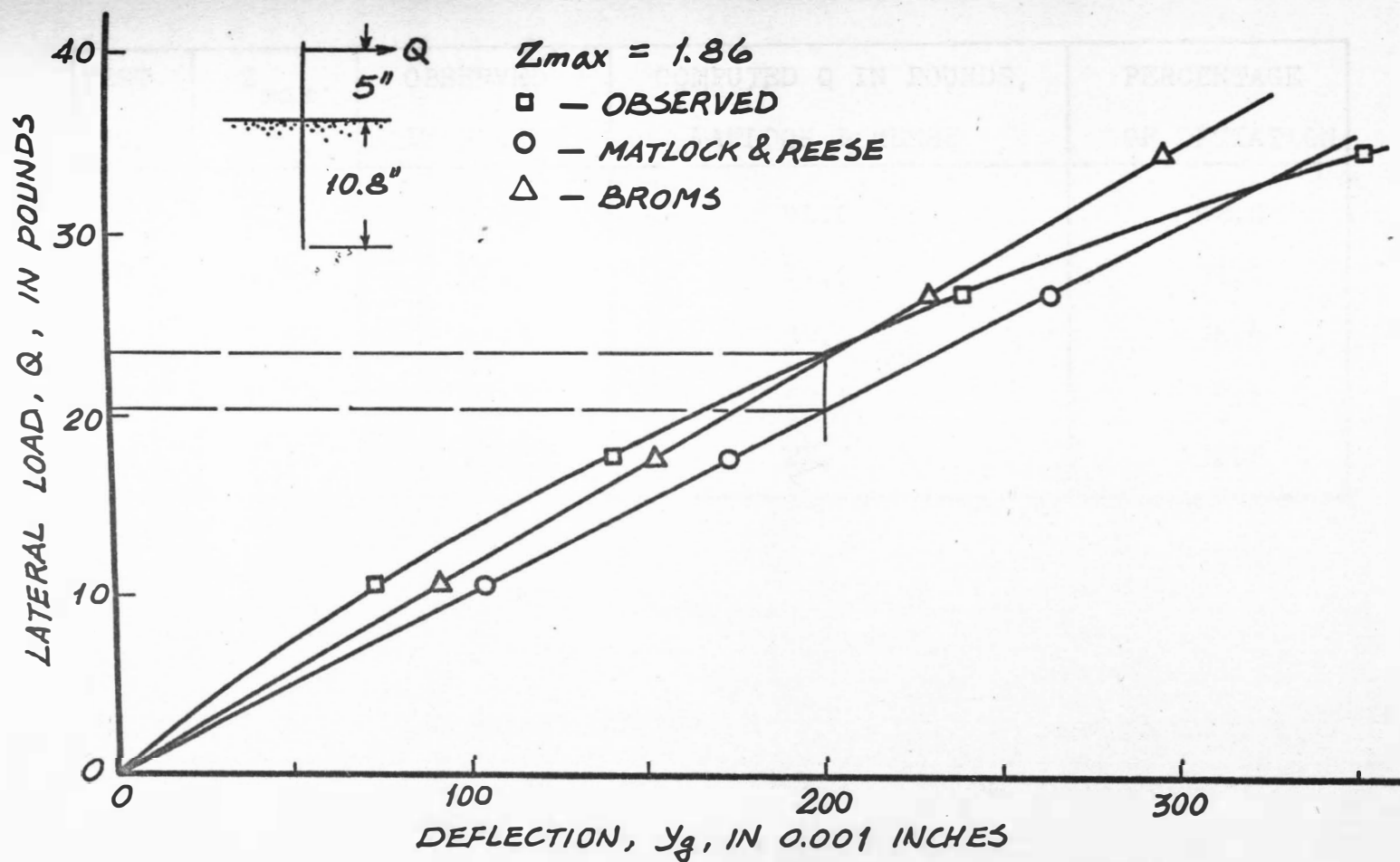


FIGURE 30. LATERAL LOAD vs DEFLECTION FOR 9/16-INCH ROUND STEEL BAR EMBEDDED IN MEDIUM DENSE SAND

TABLE 7. LATERAL RESISTANCE, Q, FOR 9/16-INCH ROUND STEEL
BARS EMBEDDED IN MEDIUM DENSE SAND

TEST NO.	Z_{\max}	OBSERVED IN POUNDS	COMPUTED Q IN POUNDS, MATLOCK & REESE	PERCENTAGE OF DEVIATION
12	5.31	70.5	41.0	42.0
13	4.45	59.5	41.0	31.1
14	3.59	54.5	39.2	28.4
15	2.72	47.3	29.5	37.6
16	1.86	23.5	20.5	12.8

presented in Figures 26 through 30. The allowable lateral loads corresponding to one-half of the critical deflection $y_g = 0.200$ inches were determined. Table 8 shows a summary of these values. The theoretical allowable lateral resistances computed by Broms' method were very close to those computed by Matlock and Reese's generalized solutions. Deviations of from 20% up to around 50% were noted between the theoretical allowable lateral loads by using Broms' method and the observed test results for Z_{max} greater than 2.72. Good agreement was obtained for a short pile with $Z_{max} = 1.86$ showing a deviation of 14.6%.

Figure 31 shows the moment diagram along the embedded portion of a 1/2-inch steel pipe surrounded by medium dense sand when subjected to lateral load. Moment curves of three different lateral loads were plotted. The observed maximum moments were found to be greater than the theoretical values computed by Matlock and Reese's method, and the deviations ranged from 7.4% up to 14.9%. The yielding moment for the test specimen was 1343 inch-pounds which corresponded to a lateral load of 118.686 pounds by interpolation. The computed ultimate lateral resistance by using Equation 21 of Broms' method is 84.2 pounds. The deviation is 29.1%. The relation of lateral load, Q , versus deflection, y_g , for the same test presented in Figure 32 shows that even though the yielding moment of the steel pile is reached, the

TABLE 8. ALLOWABLE LATERAL LOADS, Q, CORRESPONDING TO

$y_g = 0.100$ INCH FOR 9/16-INCH ROUND STEEL BARS

EMBEDDED IN MEDIUM DENSE SAND

TEST NO.	z_{\max}	OBSERVED Q IN POUNDS	MATLOCK & REESE METHOD		BROM METHOD	
			COMPUTED Q IN POUNDS	PERCENTAGE OF DEVIATION	COMPUTED Q IN POUNDS	PERCENTAGE OF DEVIATION
12	5.31	41.1	20.3	50.6	21.8	47.0
13	4.45	33.4	20.4	38.9	20.4	38.9
14	3.59	27.2	20.0	26.4	18.5	20.0
15	2.72	23.7	15.0	36.6	16.3	31.2
16	1.86	13.7	10.2	25.5	11.7	15.6

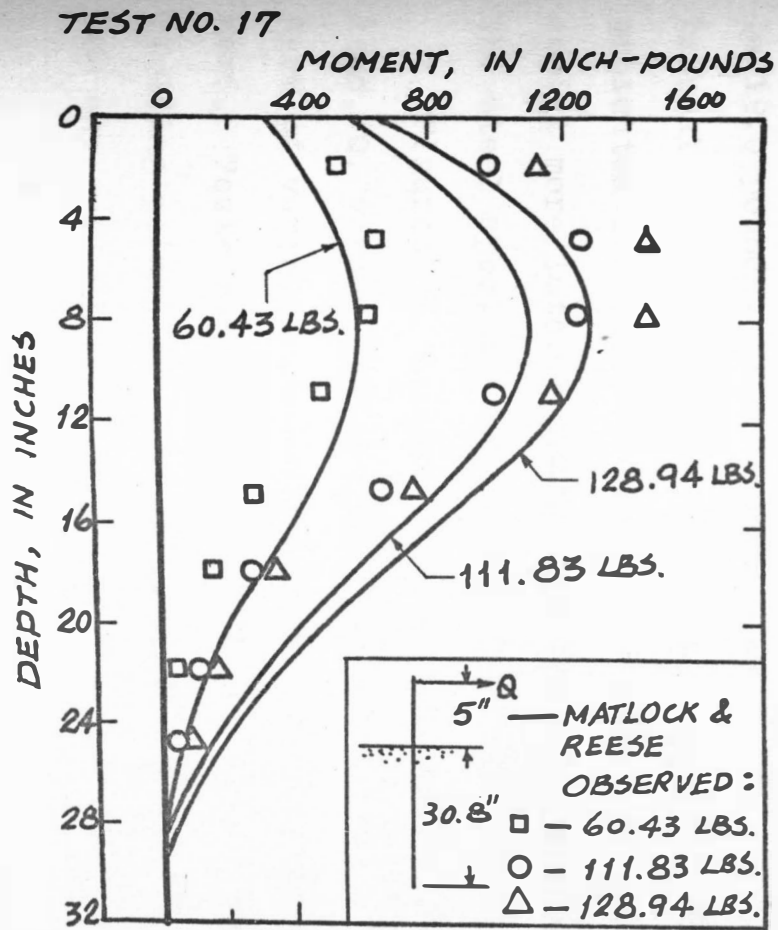


FIGURE 31. MOMENT vs DEPTH FOR 1/2-INCH STEEL TUBE EMBEDDED IN MEDIUM DENSE SAND

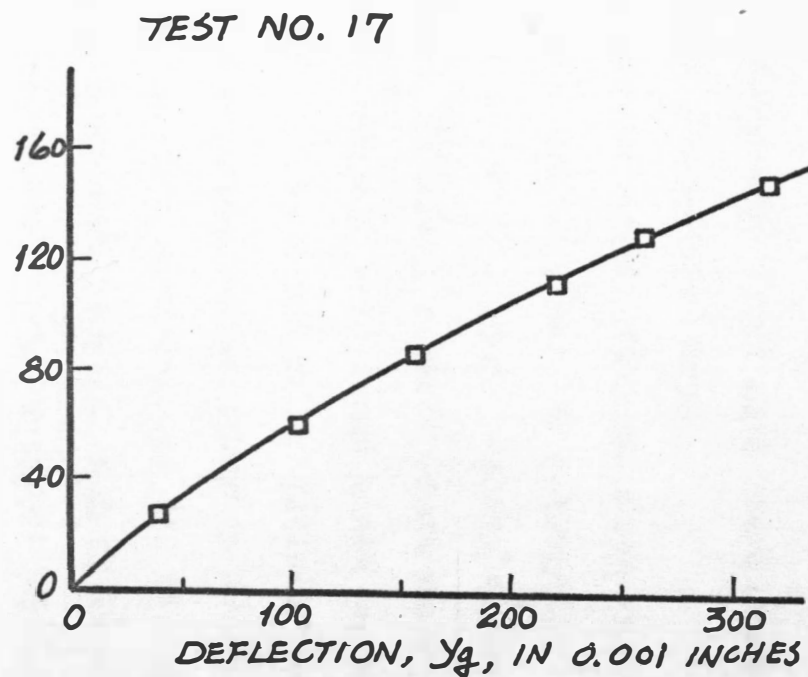


FIGURE 32. LATERAL LOAD vs DEFLECTION FOR 1/2-INCH STEEL TUBE EMBEDDED IN MEDIUM DENSE SAND

pile-soil system can still resist more lateral load. This is due to the confining soil which also contributes its ability of resisting the lateral load.

Figure 33 shows the moment diagram along the embedded portion of a 3/8-inch square steel bar surrounded by loose sand when subjected to lateral load. Moment curves resulting from three different lateral loads were plotted. The observed maximum moments were found again to be greater than the theoretical values computed by Matlock and Reese's method. The deviations ranged from 15.2% to 16.7%. The yielding moment of the test specimen was 258 inch-pounds which corresponded to an experimental lateral load of 25.26 pounds by interpolation. The computed ultimate lateral resistance by using Equation 21 of Broms' method is 19.0 pounds. The deviation is 24.8%. The relation of lateral load, Q , versus deflection, y_g , for the same test presented in Figure 34 shows that the pile-soil system can resist more lateral load, although the yielding moment of the steel specimen has already been reached.

Figures 35 through 39 show the relation of lateral load, Q , versus deflection, y_g , for 3/8-inch round steel bars of various embedment lengths surrounded by medium dense sand. Tests were carried out to the extent that an apparent yielding points of these pile-soil systems were obtainable. The observed yielding point of the pile-soil system is 47.53

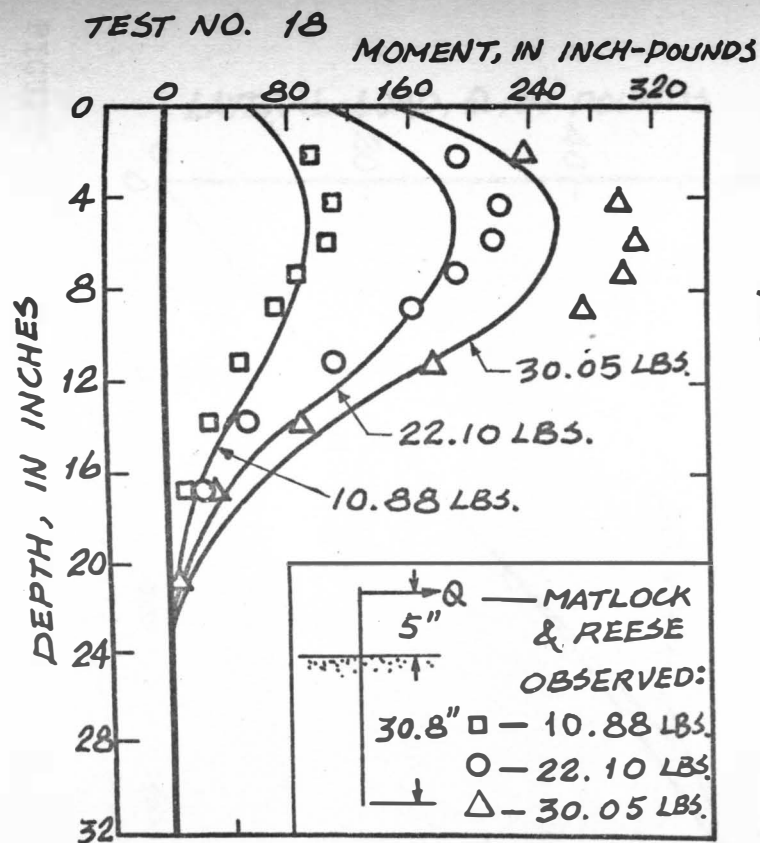


FIGURE 33. MOMENT vs DEPTH FOR 3/8-INCH SQUARE STEEL BAR EMBEDDED IN LOOSE SAND

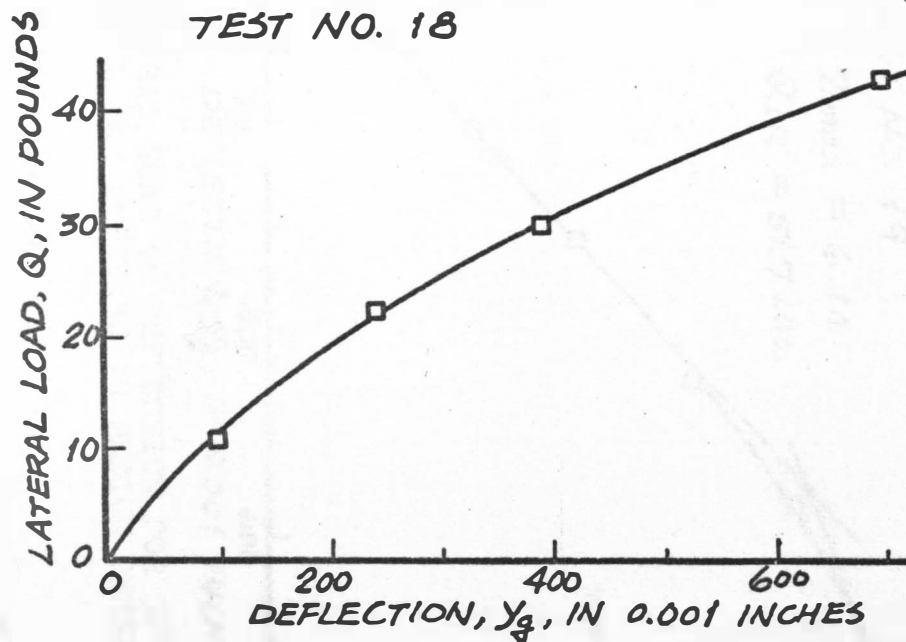


FIGURE 34. LATERAL LOAD vs DEFLECTION FOR 3/8-INCHES SQUARE STEEL BAR EMBEDDED IN LOOSE SAND

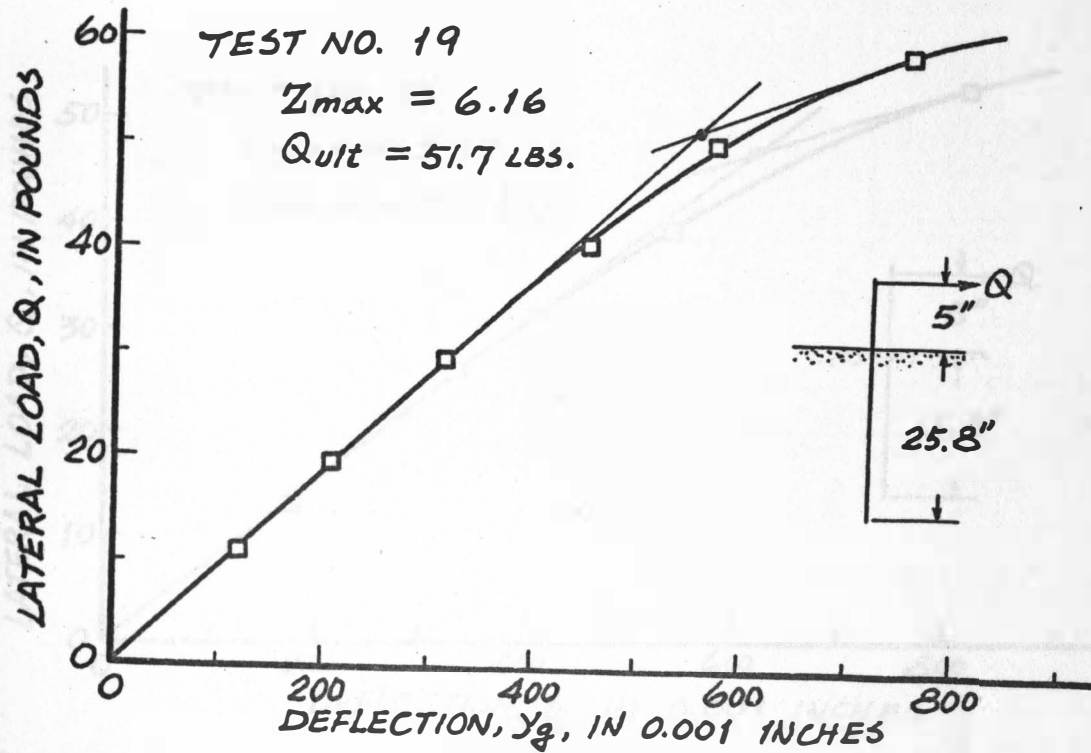


FIGURE 35. LATERAL LOAD vs DEFLECTION FOR 3/8-INCH ROUND STEEL BAR EMBEDDED IN MEDIUM DENSE SAND

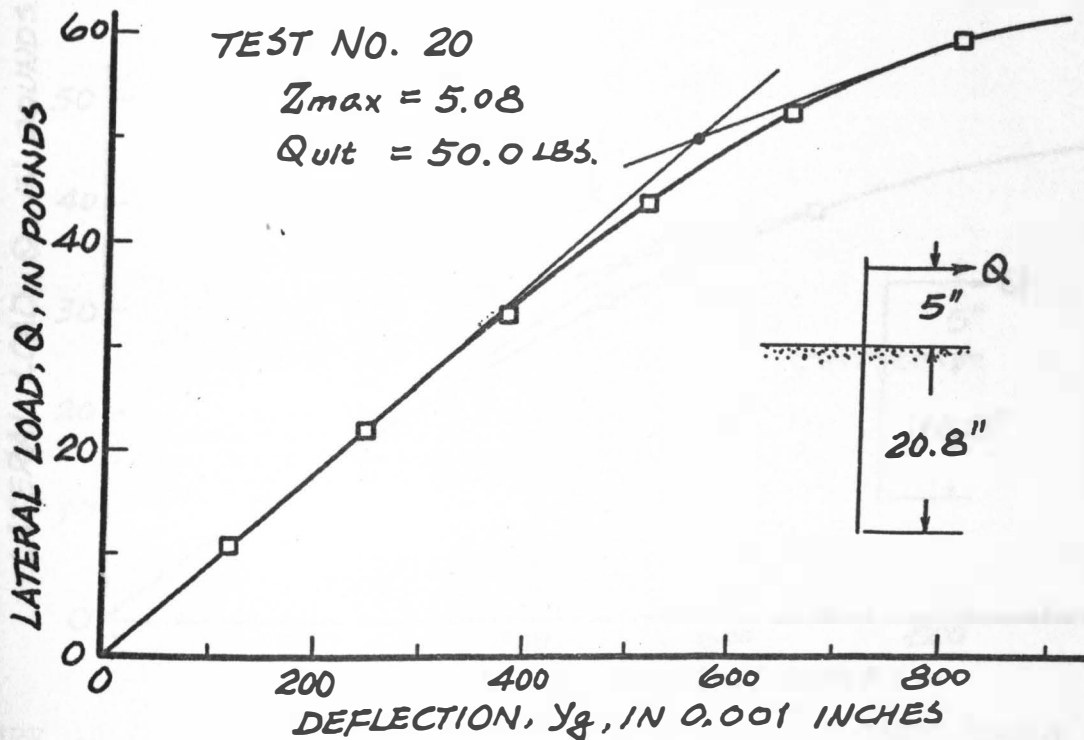


FIGURE 36. LATERAL LOAD vs DEFLECTION FOR 3/8-INCH ROUND STEEL BAR EMBEDDED IN MEDIUM DENSE SAND

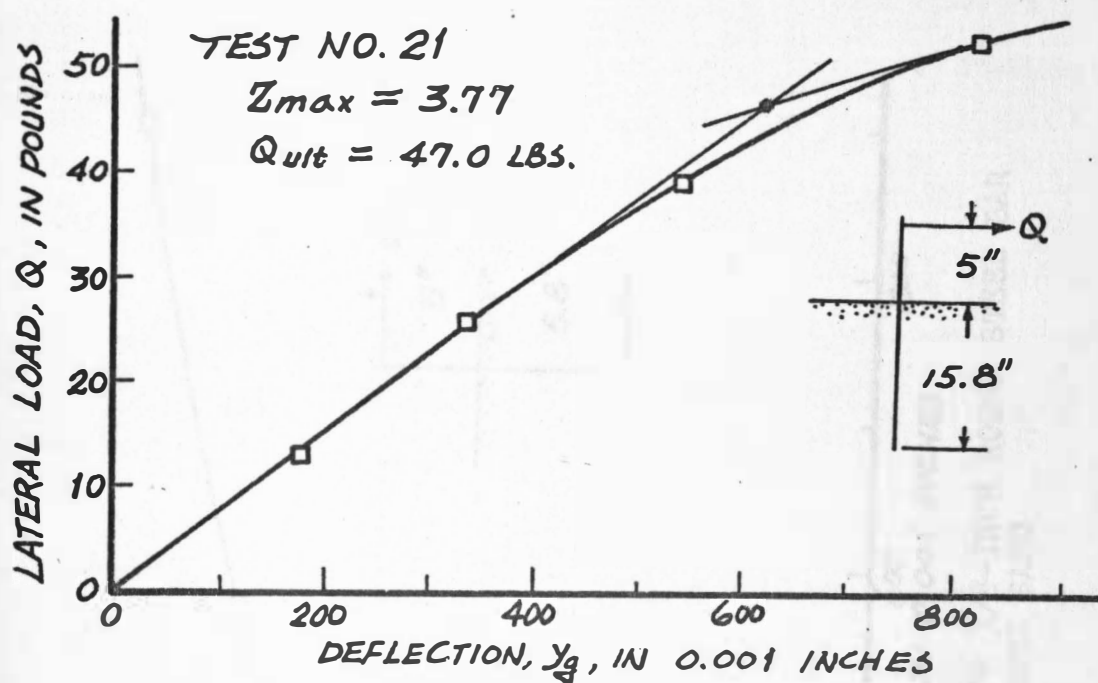


FIGURE 37. LATERAL LOAD vs DEFLECTION FOR 3/8-INCH ROUND STEEL BAR EMBEDDED IN MEDIUM DENSE SAND

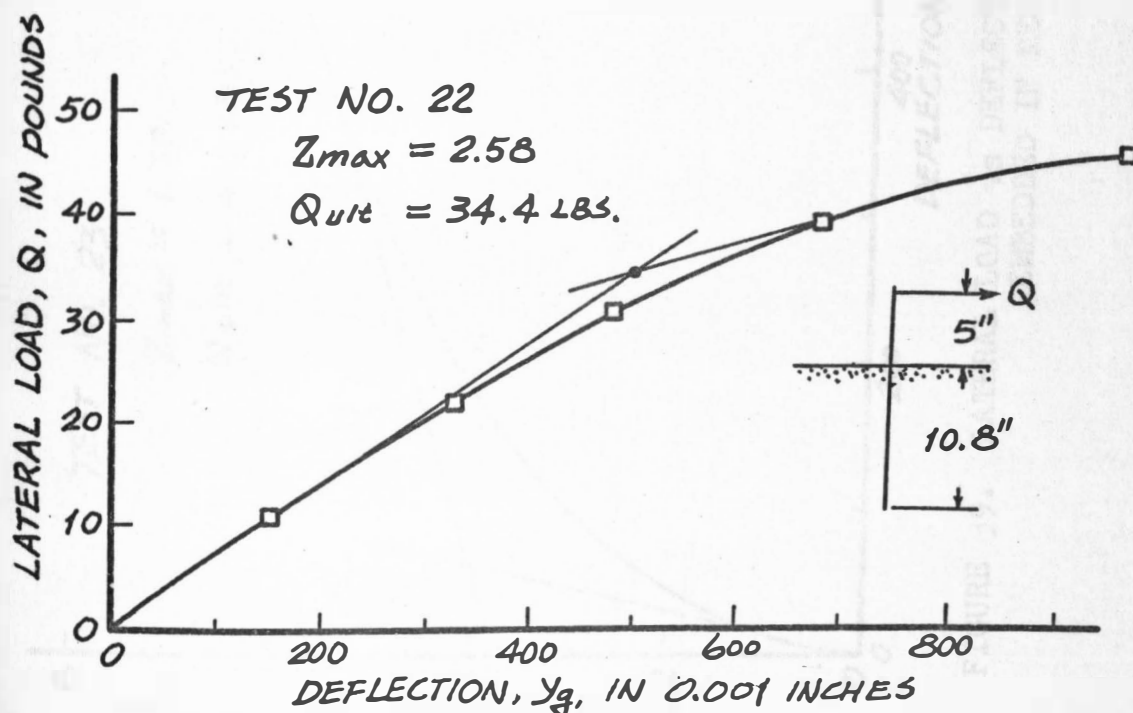


FIGURE 38. LATERAL LOAD vs DEFLECTION FOR 3/8-INCH ROUND STEEL BAR EMBEDDED IN MEDIUM DENSE SAND

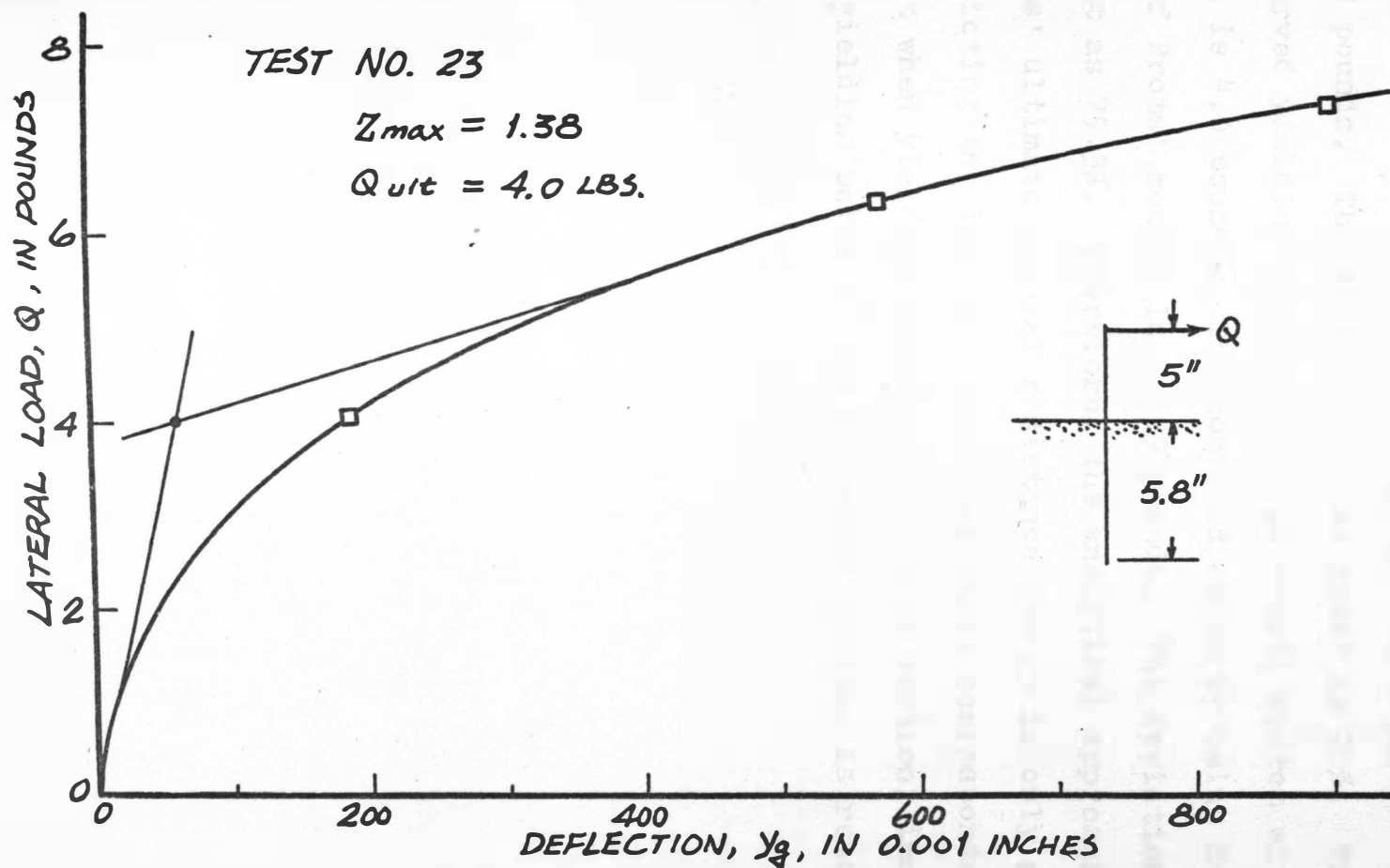


FIGURE 39. LATERAL LOAD vs DEFLECTION FOR 3/8-INCH ROUND STEEL BAR EMBEDDED IN MEDIUM DENSE SAND

pounds for $Z_{\max} = 4$ by interpolation. The computed ultimate lateral resistance by using Equation 21 of Broms' method is 14.2 pounds. The deviation is as great as 70%. The observed yielding point of the pile-soil system with $Z_{\max} = 1.38$ is 4.0 pounds. The computed value by using Equation 24 of Broms' method is 0.829 pounds. The deviation is as great as 79.3%. Therefore, the analytical approach of Broms' ultimate lateral resistance theory is only good for predicting the lateral resistance which corresponds to the point when yielding moment of the pile section, instead of the yielding point of the pile-soil system, is reached.

CONCLUSIONS

1. The linear approach by using Matlock and Reese's generalized solution to predict the lateral resistances of single free-headed piles in loose and medium sand is in general agreement with experimental results except for short rigid piles surrounded by loose sand. The theoretical results tend to be conservative. The deviation can be as great as 50%.

2. The n_h value based on initial tangent will lead to better theoretical results which are closer to experimental ones than based on an arbitrarily chosen secant when Matlock and Reese's generalized solutions are used for analytical approach.

3. $Z_{\max} \geq 4$ can be properly considered as the criterion for an infinitely long pile, although a value of 5 would be more suitable.

4. The linear approach by using Matlock and Reese's generalized solutions to predict the moments along the embedded portion of single free-headed piles surrounded by loose and medium dense sand is in general agreement with experimental results. The theoretical maximum moments are less than the experimental ones and therefore are on the unsafe side. However, the deviations are less than 20%. The fact that the pile-soil system can still resist more lateral load even when yielding moment of pile section has been

reached will compensate this defect.

5. The analytical approach by using Broms' method to predict allowable lateral loads of single free-headed piles embedded in medium dense sand is in general agreement with experimental results and is about as accurate as Matlock and Reese's generalized solutions. The theoretical results tend to be conservative and the deviation can be up to about 50%. However, the excessive conservativeness of Broms' method for piles in loose sand shows that it is less favorable than Matlock and Reese's generalized solutions.

6. The analytical approach of Broms, ultimate resistance theory is satisfactory for predicting the lateral resistance corresponding to the development of yielding moment of pile section, but not the yielding point of the pile-soil system for single free-headed piles in loose and medium dense sand.

7. The pile-soil system can still resist a substantial amount of lateral load, although the yielding moment of the pile section has been reached. This is contributed by the lateral load-resisting ability of the surrounding soil.

REFERENCES

1. Terzaghi, K., "Evaluation of Coefficients of Subgrade Reaction," Geotechnique, Vol. 5, 1955.
2. Matlock, H. and L. C. Reese, "Generalized Solutions for laterally Loaded Piles," ASCE Journal, Soil Mechanics and Foundation Division, Vol. 86, No. SM 5, October 1960.
3. Broms, B. B., "Lateral Resistance of Piles in Cohesive Soils," ASCE Journal, Soil Mechanics and Foundation Division, Vol. 90, No. SM 2, March 1964.
4. Broms, B. B., "Lateral Resistance of Piles in Cohesionless Soils," ASCE Journal, Soil Mechanics and Foundation Division, Vol. 90, No. SM 3, May 1964.
5. Feagin, L. B., "Lateral Pile Loading Tests," Transactions ASCE, Vol. 102, 1937.
6. McClelland, B. and J. A. Focht, Jr., "Soil Modulus for Laterally Loaded Piles," Transactions ASCE, Vol. 123, 1958.
7. Prakash, S., "Behavior of Pile Groups Subjected to Lateral Loads," Ph.D. thesis, University of Illinois, 1962.
8. Alizadeh, M. and M. T. Davisson, "Lateral Load Tests on Piles-Arkansas River Project," ASCE Journal, Soil Mechanics and Foundation division, Vol. 96, No. SM 5, September 1970.
9. Davisson, M. T. and J. R. Salley, "Model Study of Laterally Loaded Piles," ASCE Journal, Soil Mechanics and Foundation Division, Vol. 96, No. SM 5, September 1970.
10. Hetenyi, M., "Beams on Elastic Foundations," University of Michigan Press Ann Arbor, 1946.
11. Wilson, S. D. and D. E. Hilts, "How to Determine Lateral Load Capacity of Piles," Pile Foundation Know-how, American Wood Preserves Institute, p. 41, February 1969.

APPENDIX A. NOTATION

NOTATION	DIMENSION
C_u Half the unconfined compressive strength of cohesive soil	$[\text{FORCE}] [\text{LENGTH}]^{-2}$
D Diameter or width of pile	$[\text{LENGTH}]$
y Lateral deflection of pile	$[\text{LENGTH}]$
x Depth below ground surface	$[\text{LENGTH}]$
EI Flexural stiffness of pile	$[\text{FORCE}] [\text{LENGTH}]^{-2}$
k Horizontal subgrade modulus	$[\text{FORCE}] [\text{LENGTH}]^{-2}$
P Soil reaction	$[\text{FORCE}] [\text{LENGTH}]^{-1}$
n_h Constant of horizontal subgrade reaction	$[\text{FORCE}] [\text{LENGTH}]^{-3}$
Q_g Lateral load applied at group surface	$[\text{FORCE}]$
M_g Moment applied at group surface	$[\text{FORCE}] [\text{LENGTH}]$
Z Depth coefficient	Dimensionless
Z_{\max} Maximum depth coefficient	Dimensionless
T Relative stiffness factor	$[\text{LENGTH}]$
$\Phi(z)$ Soil modulus function	Dimensionless
A_y Deflection coefficient due to Q_g	Dimensionless
B_y Deflection coefficient due to M_g	Dimensionless
s Slope of pile	Dimensionless
A_s Slope coefficient due to Q_g	Dimensionless
B_s Slope coefficient due to M_g	Dimensionless
M Bending moment of pile section	$[\text{FORCE}] [\text{LENGTH}]$
A_m Moment coefficient due to Q_g	Dimensionless

NOTATION

DIMENSION

B_m	Moment coefficient due to M_g	Dimensionless
V	Shear force of pile section	[FORCE]
A_v	Shear coefficient due to Q_g	Dimensionless
B_v	Shear coefficient due to M_g	Dimensionless
A_p	Soil reaction coefficient due to Q_g	Dimensionless
B_p	Soil reaction coefficient due to M_g	Dimensionless
y_g	Lateral deflection of pile at ground surface	[LENGTH]
γ	Soil density	[FORCE] [LENGTH] ⁻³
k_p	Coefficient of Rankine's passive earth pressure	Dimensionless
ϕ	Internal friction angle of soil	Dimensionless
Q	Lateral load applied at somewhere above ground surface	[FORCE]
e	Distance from ground surface up to the location of Q	[LENGTH]
f	Distance from ground surface down to the pile section where M_y occurred	[LENGTH]
M_y	Yielding moment of pile section	[FORCE] [LENGTH]
Q_{ult}	Ultimate lateral load under which the yielding point of pile-soil system occurs	[FORCE]

APPENDIX B. SAND SOIL CLASSIFICATION DATA

Classification based on Unified System: SAND SP

Percent passing No. 4 sieve	100%
Percent passing No. 200 sieve	1.0%
D ₁₀	0.19mm
D ₆₀	1.03mm
C _u	6.48
C _d	0.88
Density at maximum void ratio:	97.3 pounds per foot ³
Density at minimum void ratio:	110.0 pounds per foot ³
Density during test:	
Loose Sand	99.6 pounds per foot ³
Medium Sand	104.5 pounds per foot ³
Relative density during testing:	
Loose Sand	20.0%
Medium Sand	59.6%
Internal friction angle during test:	
Loose Sand	34°
Medium Sand	37.2°

APPENDIX C. TYPICAL VALUES OF n_h

Soil Type	n_h in pounds per inch ³	
	Dry	Submerged
Sand:		
Loose	8.1	4.6
Medium	24.3	16.2
Dense	64.8	39.4
Very loose, under repeated loading		1.5
Silt:		
Very soft, organic		0.4 - 1.0
Clay:		
Very soft		2
Repeated loads		1